

Fermi National Accelerator Laboratory

FERMILAB-Pub-86/81-A
May 1986

Neutrinos from Gravitational Collapse

Ron Mayle

University of California at Berkeley

James R. Wilson

Lawrence Livermore National Laboratory

David N. Schramm

University of Chicago

ABSTRACT

Detailed calculations are made of the neutrino spectra emitted during gravitational collapse events (Type II supernovae?). Those aspects of the neutrino signal which are relatively independent of the collapse model and those aspects which are sensitive to model details are discussed. The easier-to-detect high energy tail of the emitted neutrinos has been calculated using the Boltzmann equation which is compared with the result of the traditional multi-group flux limited diffusion calculations.

Introduction

For over 20 years, it has been known that the gravitational collapse events thought to be associated with Type II supernovae and neutron star or black hole formation are copious producers of neutrinos. In fact, the major form of energy transport in these objects comes from neutrino interactions. The neutrino fluxes produced by these events are thought to be high enough that if an event occurred within the galaxy, it could be detected on Earth. Detectors to look for such events exist in the Soviet Union, in western Europe, and in the United States (e.g., Castignoli 1985).

While the general scenario for such collapse events is well established, the detailed mechanism for the ejection of the outer envelope in a supernova while the core collapses to form a dense remnant continues to be hotly debated. Therefore, most theorists working on collapse have focused on these details in an attempt to solve the mass ejection problem. As a result most of the papers in the literature have focused on internal neutrino dynamical questions rather than the detailed nature of the fluxes which might be observed by a neutrino detector on Earth. In particular, while it has been known since the early 1970's (cf. Schramm and Arnett 1974; Wilson 1971) that the average, \bar{E} , of the emitted neutrinos was $\sim 10 \text{ MeV}$, the detailed nature of the emitted spectra has not been explored since it did not affect the dynamical significance. In most numerical calculations of stellar collapse neutrino transport is treated with diffusion approximations rather than detailed microscopic spectral



analyses. This brief review will instead focus on the emitted fluxes, with a particular emphasis on what will be emitted regardless of the internal details of the collapse model and its mass ejection method. This work will present the details of work that was preliminarily reported by Schramm, Mayle, and Wilson (1985). The conclusions do not differ in substance from the earlier work of the Soviet theorists, Imshenik and Nadyoshen and their co-workers, and numerous others who have looked at the collapse problem over the last decade. (See detailed reviews and references in the book *Numerical Astrophysics* (Centrella, LeBlanc, and Bowers 1985).

After showing that the total flux of $\sim 3 \times 10^{53}$ ergs, average energies and rough time scale of seconds are basically model independent, we will show how structure on shorter time scales may be a way to resolve different models.

The emphasis in our calculations is on the high energy neutrinos which are easier to detect. Both because the cross section for neutrino interaction with baryons is proportional to ν energy squared and because the efficiency of the detector response also increases with energy. To make a detailed analysis of this high energy region we have developed a Boltzmann equation solver code to compare with the more conventional neutrino diffusion codes. In the Boltzmann equation solver, the same density, ρ , and temperature, T profile as given by the supernova code using flux limited diffusion are used but the emission absorption and scattering rates are explicitly integrated over angle distribution of radiation rather than approximated by diffusion. As will be shown, the two approaches yield neutrino luminosities which agree to within 5-10%, and average energies within 20%.

Massive Star Evolution and the Inevitability of Collapse

It has been well established in the models of Arnett (1973) and Weaver and Woosley (1983) that massive ($M \gtrsim 8M_{\odot}$) stars evolve to an onion skin configuration with a dense central Chandrasekhar mass iron core surrounded by burning layers of silicon, oxygen, neon, carbon, helium, and hydrogen. When the iron core mass exceeds the critical value, collapse inevitably occurs since no further nuclear energy can be generated within the core. As was first emphasized by Arnett and Schramm (1973) and has now been shown in great detail by Weaver and Woosley (1983) and Wilson et al. (1985), if the outer mantle and envelopes of these massive stars can be ejected, they give abundance distributions which fit remarkably well the observed "cosmic" abundances for the bulk of the heavy elements. To have such an ejection occur while allowing the core to collapse to a neutron star or black hole depends on the detailed physics of the core's equation of state and the neutrino transport of energy and momentum within the core as well as the hydrodynamics of the core. If collapse to B.H. is delayed by about a second after bounce spectra and mass ejects should not be affected by B.H. formation.

Some have argued (c.f. Bethe and Brown 1985 and Baron et al. 1985) that stars with $10 \lesssim M \lesssim 16M_{\odot}$ collapse with a small enough core mass that the shock from the core bounce leaves the core and ejects the outer envelope if the supra nuclear density matter is very soft. Stars more massive than $16M_{\odot}$ (but $\lesssim 100 M_{\odot}$ where mass loss and pair formation alters the scenario) have the shock from their bounce die before leaving the core. However, recently Wilson et al. (1985) have shown that such stars will eventually ($\lesssim 1$ second later) eject their envelope due to neutrinos generated by

accretion on the collapsing core. (This delayed ejection can also occur in the lower mass collapses if the initial bounce doesn't work.) The nucleosynthetic yields generated in this late time ejecta for the massive stars look particularly good. Obviously the above scenarios are sensitive to the stiffness of the core equation of state which is still poorly known at and above nuclear matter densities. However, independent of the details of the core bounce and mass ejection are the gross energetics of the collapse which determine the neutrino fluxes. In fact, it has been shown that even if the core undergoes convection, the net external neutrino fluxes are not significantly affected over those models without convection. (We ran the $25M_{\odot}$ Model C with a mixing length type convection and found the luminosity increased by at most 50%)

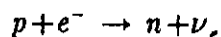
Model Independent Considerations

Regardless of the details for the collapse, it is clear that to form a neutron star, $\sim 3 \times 10^{53}$ ergs must be released. The total light and kinetic energy of a supernova outburst is $\lesssim 10^{51}$ ergs. Thus the difference must come out in some invisible form, either neutrinos or gravitational waves. It has been shown (Shapiro 1978) that gravitational radiation can at most carry away 1% of the binding energy for reasonable collapses because neutrino (Kazanas and Schramm 1976, 1977) radiation damps out the non-sphericity of the collapse before gravitational radiation. Thus the bulk ($\gtrsim 99\%$) of the 3×10^{53} ergs come off in the form of neutrinos.

It is also well established (Freedman, Schramm, and Tubbs 1977) that for densities, $\rho \gtrsim 2 \times 10^{11}$ g/cm³, the core is no longer transparent to ν 's. Thus as Mazurek (1974) first emphasized the inner core has its neutrinos in equilibrium with the matter. For electron neutrinos the neutrino "photosphere" has a temperature such that $E_{\nu} \sim 10$ MeV. This was established once it was realized that the collapsing iron core would be ~ 1 to $2M_{\odot}$ due to the role of the Chandrasekhar mass in the collapse. Since the ν_{μ} 's and ν_{τ} 's only interact at these temperatures via neutral rather than charged currents their photosphere is a little deeper within the core so their temperature is a little higher than that for ν_e 's and thus $E_{\nu_{\mu}} = E_{\nu_{\tau}} > E_{\nu_e}$ (with a similar relationship for anti-neutrinos as well).

It should also be noted that since the interaction cross sections σ are proportional to E_{ν}^2 , that lower energy ν 's can get out from deeper in the star (but deeper means fewer low energy ν 's). Thus the energy distribution of the emitted ν 's is not a pure thermal distribution for the temperature of the neutrino photosphere but can be fit at early times with an effective temperature that is a bit below the actual photospheric temperature, with the shape of the high energy end of the distribution evolving with time. This will be described in more detail later in this paper.

In addition to the above energetic arguments, there is also the basic neutronization argument. (Schramm 1976 and references therein.) The collapsing core has $\sim 10^{57}$ protons which get converted to neutrons via



to form a neutron star. Since each ν_e so emitted from the core carries away ~ 10 MeV. Then $\sim 10^{52}$ ergs are emitted by neutronization ν_e 's. This is $\lesssim 10\%$ of all the ν 's radiated. The remainder of the neutrinos come from pair processes such as

$$e^+ + e^- \rightarrow \nu_i \bar{\nu}_i$$

where $i = e, \mu$ or τ , with ν_μ and ν_τ production occurring via neutral currents and ν_e via both charged and neutral currents.

Since about a third of the neutronization occurs in the initial collapse whereas the pair ν 's come from the "thermally" radiating core, the timescale for the initial ν_e burst will be much less ($\lesssim 10^{-2}$) than the diffusion time (\sim seconds) that governs the emission of the bulk of the flux. This point has been emphasized by Burrows (1984) in a recent summary and is seen in the explicit calculations reported in this paper, as well as the earlier work of Woosley et al. (1985), Freedman et al. (1977), and Schramm (1976).

Because of the high initial temperature of the collapsing, bouncing core, about half of the pair neutrino emission comes out in the first second. In fact, the initial "thermal" neutrino luminosity is $\sim 3 \times 10^{53}$ erg/sec for the first few tenths of a second. The remaining half comes out over a few 10's of seconds as the hot newborn neutron star cools down to become a standard "cold" neutron star (Burrows and Lattimer 1985). Due to their only being emitted via neutral current processes, the luminosity of the ν_μ 's and ν_τ 's during the pair phase is less than ν_e 's but the average energy of the ν_μ 's and the ν_τ 's is slightly higher than the ν_e 's. (The ν_e luminosity, L_{ν_e} , is $\approx L_{\nu_\mu} + L_{\nu_\tau}$.)

In both the initial bounce and in the late explosive ejection models, as well as the delayed explosion models, for $8 \lesssim M \lesssim 16M_\odot$, the only distinctive structure in the neutrino signal is the initial neutronization burst. In the delayed explosion of Wilson et al. (1985) for $M \gtrsim 16M_\odot$ the first second of pair emission show repeated structure as accretion occurs with bumps in the neutrino luminosity occurring on an ~ 0.1 second timescale until the envelope ejection, at ~ 1 second, the remaining binding energy comes off smoothly with the neutrino luminosity down by a factor of 10^3 in ~ 40 seconds (Burrows and Lattimer 1985) and the average ν energy dropping from $\gtrsim 10$ MeV at 1 sec to $\lesssim 5$ MeV at 30 seconds. This means that the first ν 's emitted will be easier to detect than the final ones.

The Calculations and Results

The Appendix describes the computer codes used for both the multigroup flux limited diffusion and the Boltzmann equation solver code. Collapse models were run for the 10, 11, 12, 15, 25, 50, and $100M_\odot$ stars of Weaver and Woosley as described in Wilson et al. 1985. Models were run with different values for the $^{12}\text{C}(\alpha\gamma)^{16}\text{O}$ reaction rate.

These rate variations were classified as follows:

Model A - Fowler, Coughlan, Zimmerman 1975 rate

Model B - 2.5 times rate of Model A

Model C - 3 times rate of Model A

corresponding to Coughlan et al. 1984, as discussed by Wilson et al. (1985).

These differences of reaction rate affect the core collapse because they affect the collapsing final Fe core mass associated with the initial main sequence mass. As Wilson et al. 1985 demonstrate, the new rate gives larger cores for a given mass star. For example, the Model C $50M_{\odot}$ has a core like the Model A $100M_{\odot}$. It also alters the outer structure. Wilson et al. 1985 showed that the ejected composition with the new rate gives excellent agreement with observed elemental and isotopic abundances when the delay neutrino driven explosion is used. The neutrino emission is only dependent on the core structure. However, the initial Fe core depends upon initial stellar mass, reaction rates, and assumed convection models. After the Fe core starts to collapse, the inner homologous core begins to fall in faster. Its mass is almost independent of the initial model. The first burst of electron neutrinos comes mainly from the inner core and so is somewhat model independent. (c.f. Figures 1 and 2) with a duration of ~ 0.01 sec (see expanded scale plot of burst in Figure 1B). In the larger mass cores coming from stars with $M \simeq 20M_{\odot}$, the subsequent infall of material onto the initially collapsed core produces the additional structure seen in Figure 1A ($25M_{\odot}$; Model C) that is not seen in Figure 2 ($12M_{\odot}$; Model C). The dynamics related to this structure are clearly seen in Figure 3 where the electron neutrino emission of Figure 1 is superimposed on the dynamical tracts of the zones of the collapsing core. Figure 1A also shows the luminosity of $\bar{\nu}_e$ and ν_{μ} 's ($L_{\nu_{\mu}} = L_{\nu_{\tau}} = L_{\bar{\nu}_{\mu}} = L_{\bar{\nu}_{\tau}}$). Note that these species do not have an initial burst but otherwise show the same basic structural features, with each having a particularly high peak that causes the explosion at $t \sim 0.9$ sec. Roughly 1/3 to 1/2 of the available binding energy is emitted as ν 's in the first second, the remainder comes out over the next 10 to 20 sec.

Figure 1C shows the electron neutrino emission for a $25M_{\odot}$ Model B. Notice how this behaves similarly to a lower mass star with Model C $^{12}C(\alpha\gamma)^{16}O$ rate since the lower Model B $^{12}C(\alpha\gamma)^{16}O$ rate produces a smaller core. [$^{12}C(\alpha\gamma)^{16}O$ rates are from Fowler et al. 1975, and Caughlan et al. 1985.] Figures 4a and b show 50 and $100M_{\odot}$ stars with Model A $^{12}C(\alpha\gamma)^{16}O$ rates. Note that more massive stars have more structure. This is due to the fact that higher mass cores also have associated with them higher density envelopes. The post bounce structure is due primarily to the emission of the infalling envelope as it hits the dense core.

The time integrated energy spectrum calculated with the Boltzmann equation solver of the emitted neutrinos, antineutrinos, and mu neutrinos is shown in Figs.(6a, b, and c) for the $12M_{\odot}$ Model C case at 0.177 sec., 0.588 sec., and at *infinity*, and in Figs.(7a, b, and c) for the $25M_{\odot}$ Model C case at 0.754 sec., 0.925 sec., and at ∞ . Note that ν_{μ} 's have a far flatter high energy tail. Figs.(8a, b, c, d, and e) show a $25M_{\odot}$ Model C sequence of electron neutrino spectra at different times calculated with both the Boltzmann equation solver and the standard diffusion code. Note that at early times the diffusion code overestimates the high energy tail, but at late times the two techniques are in good agreement. The shape of the neutrino spectra is not a pure thermal distribution because neutrinos of different energies have different interaction cross sections, so the emitted neutrinos do not all come from the same temperature shell. However, as can be seen from the spectra the shape is smooth and has a modified effective thermal shape. As time goes on from the initial one-second action to the later times (~ 10 sec.), thermal neutrino cooling, results in the average neutrino energy dropping by a factor of ~ 2 (Burrows 1985). Since neutrino

detection is easier at high energies, the μ and τ neutrinos are of particular interest if detectors can be devised to pick them out via neutral current interaction; also, since the neutrino energies drop, it is no doubt easier to see the initial one-second emission at ~ 10 sec. even though the later emission accounts for over $1/2$ the binding envelope.

References

- Arnett, W.D. 1973, in *Explosive Nucleosynthesis*, (Austin: University of Texas Press).
- Arnett, W.D., and Schramm, D.N. 1973, *Ap.J.*, **184**, L47.
- Baron, E., Cooperstein, J., and Kahana, S. 1985, *Phys.Rev.Lett.*, **55**, 126.
- Bethe, H. 1986, *Phys.Rev.Lett.*
- Bethe, H., and Browne, G. May 1985, *Scientific American*.
- Bowers, R., and Wilson, J.R. 1982, *Ap.J.Suppl.*, **50**, 115.
- Burrows, A. 1984, in *Proc. Homestake Conference on Solar Neutrinos*, (Lead, South Dakota).
- Burrows, A., and Lattimer, J. 1985, talk at Aspen Center for Physics.
- C. Castignoli, ed. 1985, *Proc. 1st Int. Conf. on Underground Physcs*, San Vincent, Italy. Published in *Nuovo Cimento*.
- Caughlan, G., Fowler, W., Harris, W., and Zimmerman, B. 1985, *Ann.Rev. Astron. & Astrophys.*, in press.
- Centrella, J., LeBlanc, J., and Bowers, R., eds. 1983, *Proc. of James R. Wilson's 60th Birthday Symposium*, "Numerical Astrophysics" (Urbana,IL).
- Fowler, W., Caughlan, G., and Zimmerman, B. 1975, *Ann.Rev.Astron. and Astrophys.*, **13**, 69.
- Freedman, D.Z., Schramm, D.N., and Tubbs, D.L. 1977, *Ann.Rev.Nuc.Sc.*, **27**, 167 (and references therein).
- Fuller, G., Fowler, W., Newman, M. 1984, preprint.
- Kazanas, D., and Schramm, D.N. 1976 *Nature*, **262**, 671.
- Kazanas, D., and Schramm, D.N. 1977 *Ap.J.*, **214**, 819.
- Mazurek, T. 1974, *Astrophys. and Space Science*.
- Schramm, D.N., and Arnett, W.D. 1974, *Ap.J.*
- Schramm, D.N., Mayle, R., and Wilson, J. 1985, *Proc. 1st Int. Conf. on Underground Physics*, loc.cit.
- Schramm, D.N. 1976, *Proc. 2nd DUMAND Symposium*, (Batavia,IL: Fermilab) p. 87.
- Shapiro, S. 1978, in *Gravitational Radiation*, ed. L. Smarr (Oxford University Press).
- Smirnov, L. 1986, Inst. of Nuclear Physics preprint.
- Tubbs, D., and Schramm, D.N. 1975, *Ap.J.*, **201**, 467.
- Walker, T., and Schramm, D.N. 1986, in preparation.
- Weaver, T., and Woosley, S. 1983, in *Proc. Wilson Symposium*, loc. cit.
- Wilson, J.R. 1971, *Ap.J.*, **163**, 209.

Wilson, J.R., Mayle, R., Woosley, S., and Weaver, T. 1985, *XII Texas Symp. Rel. Ap.*, (in press).

Woosley, S., Wilson, J., and Mayle, R. 1985, *Ap.J.*, (in press).

Figure Captions

Figure 1 Neutrino luminosity versus time for two $25M_{\odot}$ progenitor stars. The stars are structurally different due to the different $^{12}\text{C}(\alpha,\gamma)^{16}\text{O}$ reaction rate used in each. Solid line is the electron neutrino luminosity, dashed is the electron antineutrino luminosity and the dash dot dot line is the muon neutrino luminosity. Note that the electron capture burst is drawn one half its actual height so that other structure is more easily seen. This does not apply to Figure 1B where the burst luminosity is shown on a magnified time scale.

Figure 2 Electron neutrino luminosity versus time for the $12M_{\odot}$ Model C.

Figure 3 Electron neutrino luminosity versus time $25M_{\odot}$ Model C superimposed onto the constant mass trajectories.

Figure 4 Electron neutrino luminosity versus time for the 50 and $100 M_{\odot}$ stars.

Figure 5 Average neutrino energies versus time for the $25M_{\odot}$ Model C.

Figure 6 Time integrated neutrino spectra taken at three different times for the $12M_{\odot}$ Model C. The area under the curves gives the total luminosity in MeV/sec.

Figure 7 Time integrated neutrino spectra taken at three different times for the $25M_{\odot}$ Model C (see caption on Fig.6 for additional detail).

Figure 8 (a - e) show comparisons of the spectrum calculated with the flux limited diffusion approximation and with the Boltzmann equation. Five times are chosen during the evolution to show the general trends. Figure 1a is 0.1 second after bounce, while figure 1b is just before the explosion. Figure 1c is at the explosion time. These three figures show the most discrepancy between the two methods, and are all taken when there is unsteady motion in the atmosphere. Figures 1d and 1e show times after explosion when matter motion is fairly steady on one second timescales. Here agreement is very good.

APPENDIX

Neutrino Transport

The supernova computer code transports electron neutrinos using multigroup flux limited diffusion. The following equation determines the neutrino evolution.

$$\frac{dF}{dt} = \nabla \cdot (D \nabla F) + \frac{dF}{dt_{cap}} + \frac{dF}{dt_{comp}} + \frac{dF}{dt_{scatt}} + \frac{dF}{dt_{ea}} + \frac{dF}{dt_{rad}} \quad (1)$$

where the energy density of electron neutrinos at $r = \int_0^\infty F(E, r) dE$ and D is the diffusion coefficient. D contains a flux limiter that forces $F(E, r)$ to be proportional to $1/r^2$ in regions where neutrinos are free-streaming. The form used for D is as follows:

$$D = \frac{\lambda c}{3 + \lambda \left| \frac{d \ln F}{dR} \right| \xi} \quad (2)$$

where

$$\xi = 1 + \frac{3}{1 + \frac{x}{2} + \frac{x^2}{8}} ; \quad x = \lambda \left| \frac{d \ln F}{dR} \right| \quad (3)$$

The terms on the right hand side of (1) represent changes in the neutrino field due to diffusion, electron capture, changes in volume, scattering, emission and absorption, and work done on matter.

The electron antineutrinos and mu-tau neutrinos and antineutrinos are similarly treated except that the capture term is not included. See Bowers and Wilson (1982) for a detailed discussion of the transport used.

In order to check on the accuracy of the high energy part of the electron neutrino spectrum calculated by the supernova code, another method of neutrino transport was used. This new method solves the Boltzmann transport equation and therefore takes into account the angular distribution of the neutrinos. However, the density, temperature, and composition profiles given by the supernova code with the flux limited diffusion approximation are used to construct opacities for the neutrino interactions. We felt this would be an acceptable approximation to the extent that the two methods give similar results. More on the validity of the results will be said later after a description of the Boltzmann transport equation and a discussion of the results obtained by the calculation.

Boltzmann Transport Equation

Let f represent the distribution function of electron neutrinos such that

$$\int f(\vec{x}, \vec{p}, t) \frac{d^3 p}{h^3} = \text{number density of neutrinos} \quad (4)$$

In the limit of complete thermodynamic equilibrium:

$$f(\vec{x}, \vec{p}, t) = \frac{1}{\exp\left(\frac{E-\mu}{kT}\right)+1} \quad (5)$$

The transport equation for $f(\vec{x}, \vec{p}, t)$ is taken to be:

$$\begin{aligned} \frac{1}{c} \frac{\partial f}{\partial t} + \hat{p} \cdot \nabla f = & \kappa_a \rho (b - f) - f \int (1 - \tilde{f}) \rho \kappa_s(E, \Omega \rightarrow \tilde{E}, \tilde{\Omega}) \frac{d^3 \tilde{p}}{h^3} \\ & + (1 - f) \int \tilde{f} \rho \kappa_s(\tilde{E}, \tilde{\Omega} \rightarrow E, \Omega) \frac{d^3 \tilde{p}}{h^3} \end{aligned} \quad (6)$$

On the right hand side of (6), the first term represents absorption and emission of neutrinos by free nucleons, and b is a Fermi-Dirac distribution function representing emission with $\mu_\nu = \epsilon_N - \epsilon_P + \mu_e$. The second and third terms represent scattering by free nucleons, electrons and positrons, and helium nuclei.

We will only be concerned with the neutrino transport after bounce, at which time only the above sources of opacity are considered important since the heavy nuclei are all disassociated. This occurs in the region of the star from the center to well outside the neutrinosphere at the times we are solving the new transport equation. We also include helium as an opacity source since there is a small region inside the neutrinosphere very late in the collapse, where nuclear matter is around 30% helium and 70% free neutrons and protons.

Equation (6) neglects Doppler shift, Doppler aberration effects, advection, and gravitational redshift. We only used this transport method after bounce when the core is quasi-static and all the above effects are small except for the gravitational redshift. The gravitational redshift is taken into account after the final spectrum is solved for by using the energy shift that neutrinos would undergo if emitted from the neutrinosphere.

Opacities

We now estimate the importance of electron-positron scattering opacity, κ_e^s , as compared to the total opacity (helium will be ignored as an opacity source in the following derivation).

$$\frac{\kappa_e^s}{\kappa_{tot}} = \frac{n_e - \sigma_{e-\nu} + n_e + \sigma_{e+\nu}}{n_N \sigma_{N\nu} + n_N \sigma_{N\nu}^s + n_P \sigma_{P\nu}^s + n_e - \sigma_{e-\nu} + n_e + \sigma_{e+\nu}} \quad (7)$$

where

$$\sigma_{N\nu}^s \approx \left(\frac{1+3\alpha^2}{4} \right) \sigma_o \left(\frac{E}{m_e c^2} \right)^2 \quad (8)$$

$$\sigma_{N\nu}^s \approx \sigma_o (1 - C_A)^2 \left(\frac{E}{m_e c^2} \right)^2 \quad (9)$$

$$\sigma_{P\nu}^s = \frac{\sigma_o}{4} [(C_V - 1)^2 + 3\alpha^2 (C_A - 1)^2] \left(\frac{E}{m_e c^2} \right)^2 \quad (10)$$

and $\sigma_0 = 1.7 \times 10^{-44} \text{ cm}^2$, E is the neutrino energy. If $C_V \simeq 1$, $C_A = 1/2$, then $\sigma_{P\nu} \simeq \sigma_{N\nu}^*$ (since $\alpha \simeq 1.2$). For the number of pairs the following holds:

$$n_{\text{pairs}} = n_{e^+} = \int \frac{1}{\exp\left(\frac{e+\mu_e}{kT}\right)+1} \frac{d^3p}{h^3} \approx \frac{1}{\pi^2} \left(\frac{m_e c}{h}\right)^3 \left(\frac{kT}{m_e c^2}\right)^3 F_2^-(\eta) \quad (11)$$

(True if $\frac{m_e c^2}{kT} \ll 1$)

where

$$F_2^-(\eta) = \int_0^\infty \frac{x^2 dx}{e^{x+\eta}+1}; \quad \eta = \frac{\mu_e}{T} \text{ and } T \text{ is measured in MeV} \quad (12)$$

Now $F_2^-(\eta) \simeq 2e^{-\eta}$ is an approximation good to within 10% (see Fuller, Fowler, Newman 1984).

In the limit of degenerate electrons with $C_V=1$, $C_A=1/2$:

$$\sigma_{e-\nu} = \frac{7}{32} \sigma_0 \frac{E_{\mu e}}{(m_e c^2)^2} \quad (13)$$

If the electrons are degenerate, the number of positrons is negligible. In this limit:

$$\frac{\kappa_e^*}{k_{\text{tot}}} = \frac{\frac{7}{32} Y_e}{(1.33(1-Y_e)+.25) \frac{E}{\mu_e} + \frac{7}{32} Y_e} \quad (14)$$

In this case $\langle E \rangle \approx \mu_e$ and taking $Y_e \approx 1/3$

$$\frac{\kappa_e^*}{k_{\text{tot}}} = 06 \quad (15)$$

So electron scattering is completely negligible in the degenerate limit.

If electrons and positrons are relativistic and non-degenerate then taking $C_V=1$, $C_A=0.5$)

$$\sigma_{e-\nu} = \frac{7}{8} \sigma_0 \frac{EkT}{(m_e c^2)^2}; \quad \sigma_{e+\nu} = \frac{3}{8} \sigma_0 \frac{EkT}{(m_e c^2)^2} \quad (16)$$

Therefore in the limit of relativistic non-degenerate electrons and positrons

$$\frac{\kappa_e^*}{k_{\text{tot}}} = \frac{\frac{5.5}{\rho_7} T^3 e^{-\eta} + \frac{7}{8} Y_e}{[1.33(1-Y_e)+0.25] \frac{E}{T} + \frac{5.5}{\rho_7} T^3 e^{-\eta} + \frac{7}{8} Y_e} \quad (17)$$

There is another effect that should be accounted for in the above. The scattering opacities should be transport opacities (opacities weighted by the factor $1-\cos\theta$, where θ is the scattering angle). Using a fit taken from Tubbs and Schramm (1975) for $\cos\theta$, the above formula for the ratio of opacities can be changed to include this factor. The formula we use is:

$$\langle \cos\theta \rangle = \frac{E}{4kT + \mu_e + E} \quad (18)$$

It can be seen that if $E \gg 4kT + \mu_e$, then the electron-positron scattering will also not be important.

To estimate the value of (3) use the fact that $Y \approx 1/3$, $E \approx 3kT$, and that the electrons are slightly degenerate ($\eta \simeq 1/3$) to find:

$$\frac{\kappa_e^s}{k_{tot}} = \frac{\frac{4.3}{\rho_7} T^{3+.29}}{3.4 + \frac{4.3}{\rho_7} T^{3+.29}} \quad (19)$$

Demanding that this be less than 0.20 results in the condition $\rho_7 > 8T^3$, with T in MeV. This condition is fulfilled in the region we wish to apply the new transport method. Since nucleons dominate the opacity, the electron-positron scattering may be approximated without greatly effecting the calculated spectrum. We now give an approximate treatment of the electron scattering opacity used in the Boltzmann equation.

From the above estimate on opacity it is seen that

$$\kappa_e^s(\mu_e, T, E) = EH(\mu_e, T, E) \quad (20)$$

where $H(\mu_e, T, E)$ is a more slowly varying function of E than $\kappa_e^s(\mu_e, T, E)$ (see Tubbs and Schramm). Now write

$$f \int (1 - \tilde{f}) \kappa_e^s(E, \Omega \rightarrow \tilde{E}, \tilde{\Omega}) \frac{d^3 \tilde{p}}{h^3} = \kappa_e^s \langle 1 - \tilde{f} \rangle f \quad (21)$$

where $\langle 1 - \tilde{f} \rangle$ is some average blocking factor.

The other term involving electron-positron scattering will be approximated in such a way that in the limit $f = e^{-\frac{\mu_e - E}{T}}$, the electron-positron scattering terms will cancel (with the neglect of blocking factors). This condition results in:

$$(1 - f) \int \tilde{f} \kappa_e^s(\tilde{E}, \tilde{\Omega} \rightarrow E, \Omega) \frac{d^3 \tilde{p}}{h^3} = \frac{E}{4\pi kT} (1 - f) \int_E^\infty \int_{4\pi} \kappa_e^s(\mu_e, T, \tilde{E}) \frac{\tilde{f}}{\tilde{E}} d\tilde{E} d\tilde{\Omega} \quad (22)$$

To show this is correct, we need to do the integrals on the right hand side of the above equation with $f = e^{-\frac{\mu_e - E}{kT}}$. To do the energy integral, we take $H(\mu_e, T, E)$ outside the integral so that:

$$\frac{E}{4\pi kT} \int_E^\infty \int_{4\pi} \kappa_e^s(\mu_e, T, E) e^{-\frac{\mu_e - \tilde{E}}{kT}} \frac{d\tilde{E}}{\tilde{E}} d\tilde{\Omega} = \frac{H(\mu_e, T, E) E}{kT} \int_E^\infty e^{-\frac{\mu_e - \tilde{E}}{kT}} d\tilde{E} = \kappa_e^s f \quad (23)$$

this is a very good approximation in the limit $\frac{\mu_e}{kT} \ll 1$ since in this case, $\kappa_e^s \propto E$ and $H(\mu_e, T, E)$ is independent of E . This is also the region where $f = e^{-\frac{\mu_e - E}{kT}}$, if neutrinos are in equilibrium.

The nucleon scattering terms are simpler in form since the scattering is conservative. The proton differential cross-section has an angular dependence such that:

$$\frac{d\sigma}{d\Omega} \propto \left(1 - \frac{1}{3}\cos\theta\right) \quad (24)$$

The neutron cross-section is isotropic (see Tubbs and Schramm 1975). The nucleon scattering terms will be written as:

$$-(1-f)k_s^{N+P}f + (1-f)k_s^{N+P}\frac{1}{4\pi}\int_{4\pi}\tilde{f}d\tilde{\Omega} \quad (25)$$

where the angular dependence of the cross-section has been averaged over 4π , weighted by $(1-\cos\theta)$ in order to produce a transport cross-section. Notice that this is another approximation as the angular dependence of the cross-section really should appear inside the integral over f .

The scattering cross-section for helium is taken from Tubbs and Schramm and is given by the following expression:

$$\sigma_{He} = \frac{8}{3}\sigma_o\left(\frac{E}{m_e c^2}\right)^2 \sin^4\theta_w \quad (26)$$

For all the numerical results presented here, the value of $\sin^2\theta_w$ is 0.21.

Since both helium and neutron-proton scattering have the same dependence on the neutrino energy, the scattering opacity for these may be added to find a total conservative scattering opacity for use in the transport equation.

Boltzmann Equation Rewritten

$$\begin{aligned} \hat{p}\cdot\nabla f \Rightarrow & k_a^{N+P}(b-f) - \rho\kappa_e^e \langle 1-\tilde{f} \rangle f + \frac{E(1-f)}{4\pi k T} \int_E^\infty \int_{4\pi} \rho\kappa_e^e \frac{\tilde{f}}{E} d\tilde{E}d\tilde{\Omega} \\ & - (1-f)\rho k_s^C f + (1-f)\rho k_s^C \frac{1}{4\pi} \int_{4\pi} \tilde{f}d\tilde{\Omega} \end{aligned} \quad (27)$$

where:

$$k_s^C = k_s^{N+P} + k_s^{He} \quad (28)$$

Next, introduce a new distribution function $F(\vec{x}, \hat{p}, E)$ such that

$$F(\vec{x}, \hat{p}, E) = \left(\frac{E}{hc}\right)^3 f(\vec{p}, \vec{x}) \quad (29)$$

This is done since the supernova code uses the angular average of $F(\vec{x}, \hat{p}, E)$ as the neutrino distribution function (i.e., $F_{code} = \int F(\vec{x}, \hat{p}, E) d\Omega$).

The transport equation for $F(\vec{x}, \hat{p}, E)$ becomes:

$$\begin{aligned} \hat{p}\cdot\nabla F \Rightarrow & k_a^{N+P}(B-F) - \rho\kappa_e^e \langle 1-\tilde{f} \rangle F + \frac{E^4}{4\pi k T}(1-f) \int_E^\infty \int_{4\pi} \rho\kappa_e^e \frac{\tilde{F}}{\tilde{E}^4} d\tilde{E}d\tilde{\Omega} \\ & - (1-f)\rho k_s^C F + (1-f)\rho k_s^C \frac{1}{4\pi} \int_{4\pi} \tilde{F}d\tilde{\Omega} \end{aligned} \quad (30)$$

where $B = \frac{E^3}{(hc)^3} b$

The blocking factors $\langle 1 - \tilde{f} \rangle$ and $(1 - f)$ are evaluated using the value of f obtained from the supernova code.

The supernova code used 16 energy bins and we have used:

$$\langle 1 - \tilde{f} \rangle = \frac{\sum_{bins} \left(1 - \frac{F(\tilde{E}, \tilde{x})}{4\pi \tilde{E}^3} (hc)^3 \right) \tilde{E}^2 \Delta \tilde{E}_{bin}}{\sum_{bins} E^2 \Delta \tilde{E}_{bin}} \quad (31)$$

and

$$1 - f = 1 - \frac{F(E, \bar{x})}{4\pi E^3} (hc)^3 \quad (32)$$

We ran one collapse problem (15 M_{\odot} Model C) with 32 energy bins and found weak sensitivity in the calculated spectrum to bin number.

Equation (30) is still difficult to solve since it is a differential-integral equation for $F(\hat{p}, E, \bar{x})$. In the spirit of the preceding approximations we use the code values of the spectrum to evaluate the integral involving electron scattering since it is much less important than the nuclear contribution. We finally arrive at:

$$\hat{p} \cdot \nabla F = (k_a + k_s) \rho F + S \quad (33)$$

where

$$k_s = \kappa_e^s \langle 1 - \tilde{f} \rangle + k_e^C (1 - f) \quad (34)$$

$$S = \rho k_a B + \frac{E^4}{4\pi k T} (1 - f) \int_E^{\infty} \int_{4\pi} \kappa_e^s \rho \frac{F_{code}}{\tilde{E}^4} d\tilde{E} d\tilde{\Omega} + (1 - f) \rho k_e^C \frac{1}{4\pi} \int \tilde{F} d\tilde{\Omega} \quad (35)$$

Solution of the Transport Equation

The equation is solved iteratively with old values of F used in the angular integral in S for the next calculation of F . The iteration is terminated when the solution has converged.

Assuming S is known, equation (33) can be solved by picking a beam direction and integrating along the beam. The beams are chosen to be chords through the star, where the chords are characterized by the point of closest approach z , and x is the distance along the chord. For a problem with spherical symmetry (which we are considering) knowledge of $F(x, z, E)$ for these special beams is equivalent to knowledge of $F(r, \theta, E)$ or the angular distribution of F at a point r from the center of the star.

Calling $(k_a + k_s) \rho = 1/\lambda$, the solution of:

$$\frac{\partial F}{\partial x} = \frac{F}{\lambda} + S \quad (36)$$

is

$$F(x + \delta, z, E) = \exp\left[-\int_x^{x+\delta} \frac{dx'}{\lambda'}\right] \left[\int_x^{x+\delta} S(x', z, E) \exp\left(\int_x^{x'} \frac{d\tilde{x}}{\lambda}\right) dx' + F(x, z, E) \right] \quad (37)$$

If F, S, λ are constant over the interval $[x, x+\delta]$, then

$$F(x+\delta, z, E) = \exp\left[-\frac{\delta}{\lambda}\right] F(x, z, E) + \lambda S(1 - e^{-\frac{\delta}{\lambda}}) \quad (38)$$

This equation together with the boundary condition $F(-\sqrt{R^2 - z^2}, z, E) = 0$, with $R =$ maximum radius considered, is used to numerically integrate (33). From symmetry we only need cover the region from $z=0$ to $z=R$. We did this with about 50 beams on the average.

We feel that the errors introduced by the numerical integration are negligible compared to the uncertainty in the density, temperature, composition profile used in the opacity construction.

Electron Antineutrinos

Electron antineutrinos are treated similarly to the electron neutrinos, the only difference being the values of C_V and C_A (see Bowers and Wilson 1982). Electron-positron scattering is more important for electron antineutrinos than neutrinos since, while both types scatter off nuclei, antineutrinos are absorbed only by protons, neutrinos only by neutrons, and the value of Y_p can drop as low as 0.1 in the region near the neutrinosphere. Therefore, the approximate form for the electron scattering term in the Boltzmann equation will have a greater effect on the electron antineutrino spectrum than on the electron neutrino spectrum. However, the supernova code includes the effects of electron scattering with a more consistent approximation than that used in the Boltzmann equation, and we obtain relatively good agreement between the flux limited diffusion calculation and the calculation done with the Boltzmann equation.

Mu Tau Neutrinos and Antineutrinos

Mu tau neutrinos and antineutrinos (which we treat as four essentially identical neutrinos) are scattered but not absorbed by nucleons. The electron-positron opacity is now comparable to the baryon opacity. We did not attempt to solve for a spectrum of these with the Boltzmann equation since the electron scattering opacity was only approximated there. However, with good agreement of the electron antineutrino spectrum calculated with the supernova code and Boltzmann equation, and with the fact that electron scattering can be an important source of opacity for electron antineutrinos, we feel that the supernova code calculated mu tau neutrino spectrum is done adequately.

Recent work on neutrino mixing in the sun as a possible solution to the solar neutrino problem (Smirnov 1986 and Bethe 1986) has important implications for neutrino emission from supernova. In these models, neutrinos change into other neutrino species as they traverse matter. Thus, the higher energy $\nu_\mu, \bar{\nu}_\mu, \nu_\tau$ and $\bar{\nu}_\tau$ emitted during collapse could be partially transformed into easier to deflect ν_e 's and $\bar{\nu}_e$'s. A detailed exploration of this is being carried out by Walker and Schramm (1986).

Comments on Results

We found good agreement between the spectrum as calculated by the Boltzmann equation and by the supernova code, as average energies calculated using both spectra were within 20% of each other. The luminosities, however, were in better agreement, between 5-10%. The peak discrepancies are in the models which had the most motion in the atmosphere. (If the flux from the new method were actually fed back into the evolution equations for the star, the system would adjust so as to lower this discrepancy. For example, too high a flux would lower the temperature, thereby bringing down the flux. We estimate the discrepancy would be about one-half of what we found, taking this effect into account.)

25 M_⊙ MODEL C NEUTRINO LUMINOSITY

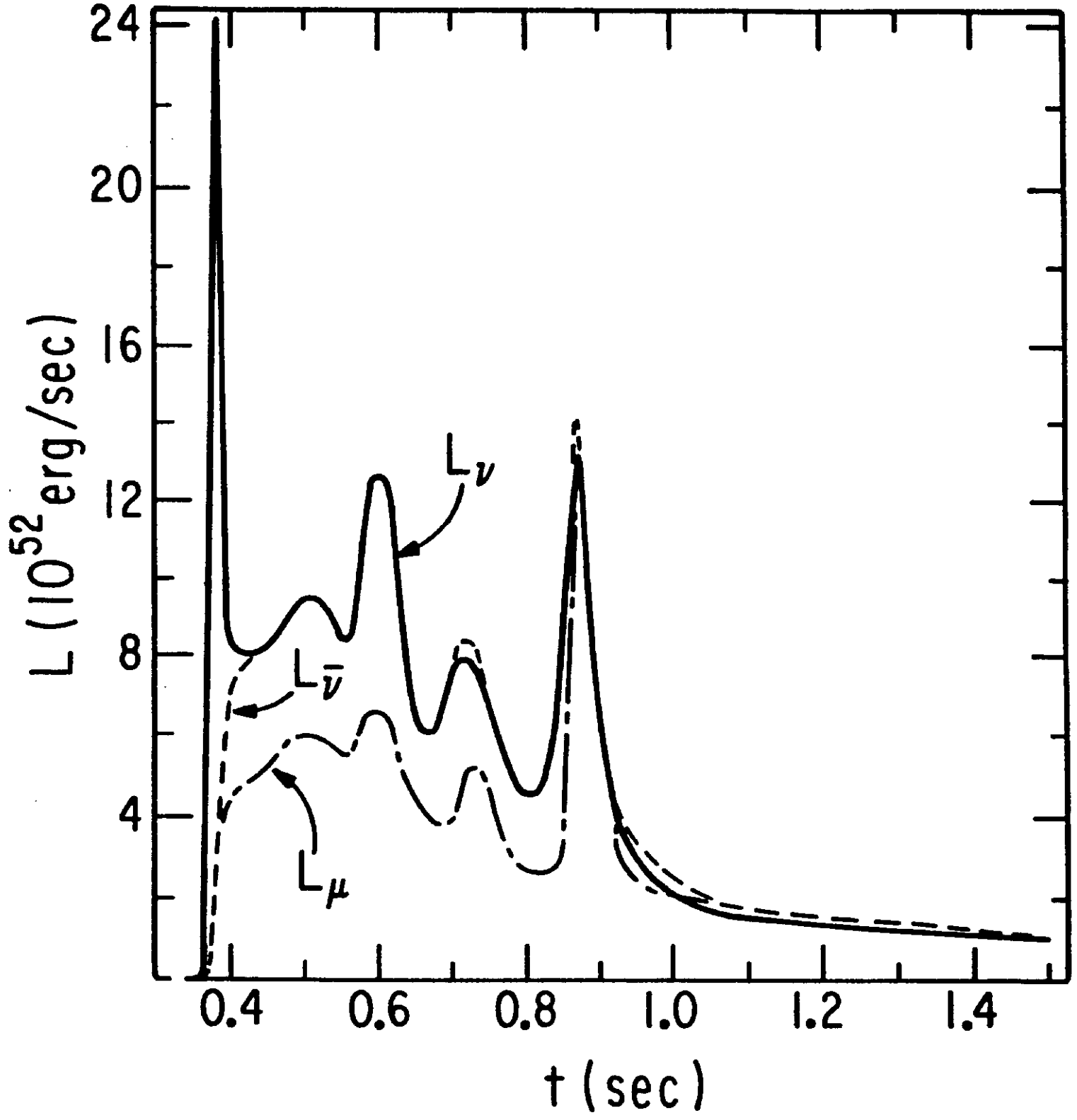


Figure 1a

25 M_⊙ MODEL C
ELECTRON NEUTRINO BURST

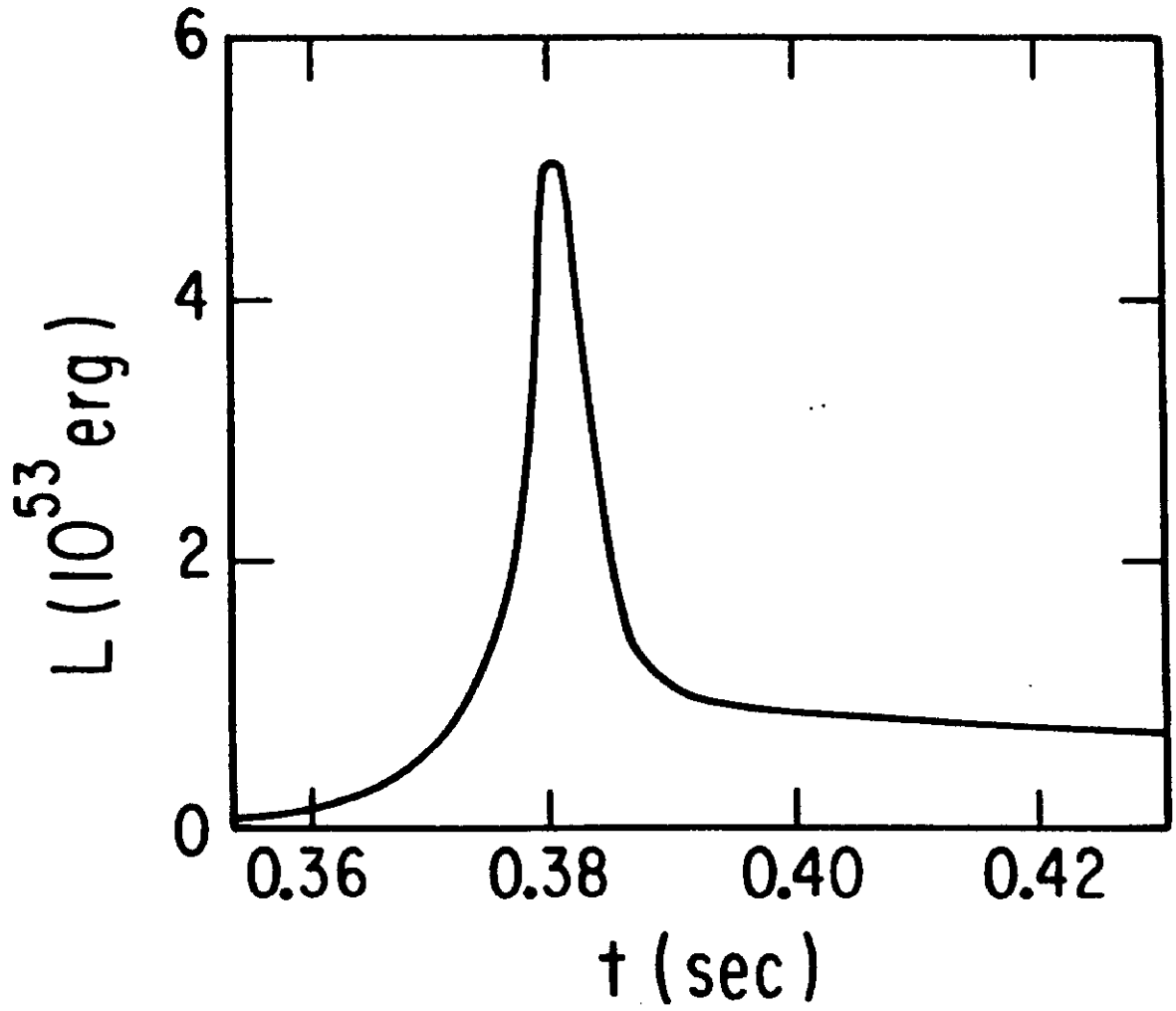


Figure 1b

25 M_⊙ MODEL C ELECTRON NEUTRINO LUMINOSITY

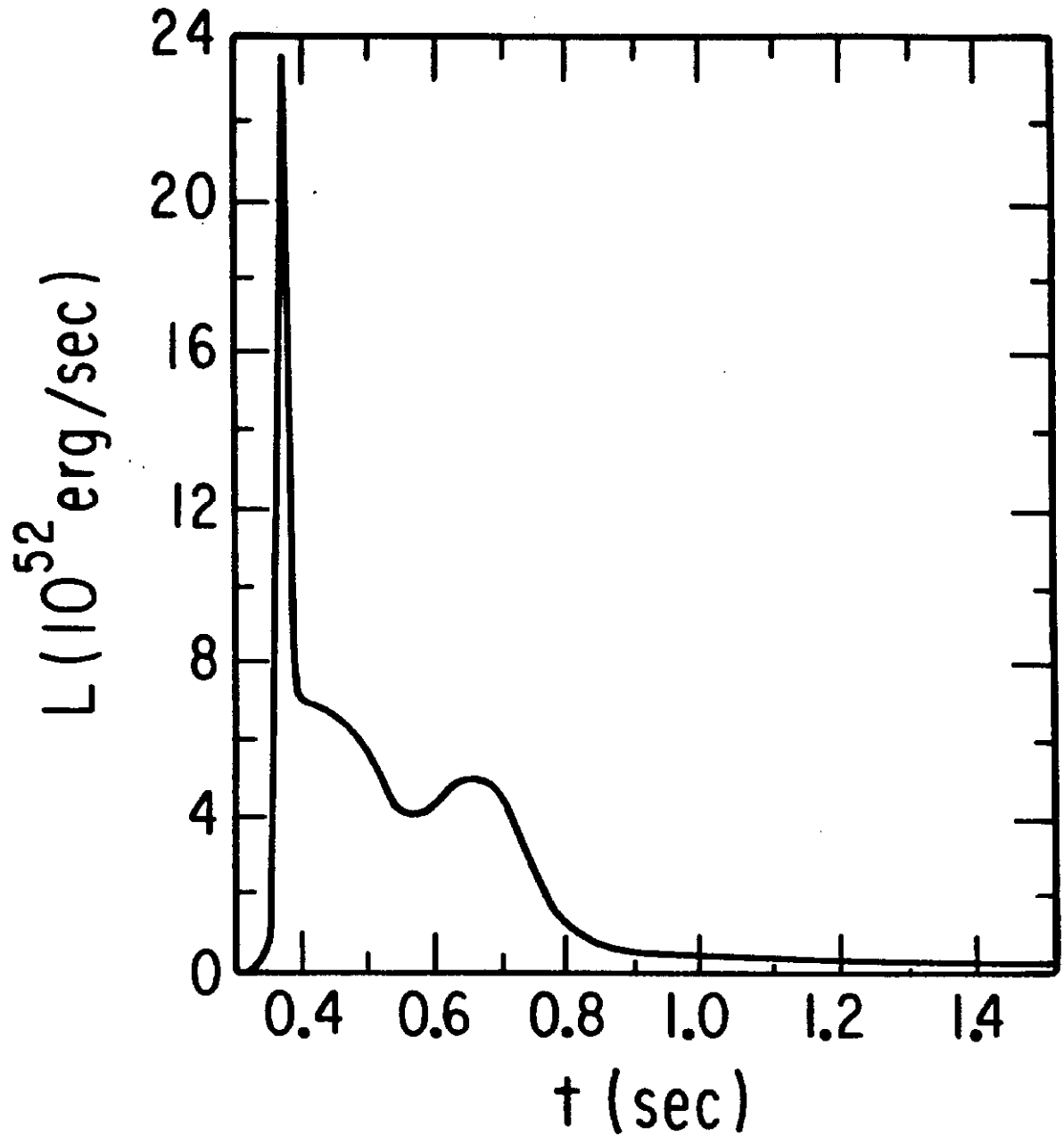


Figure 1c

12 M_⊙ MODEL C ELECTRON NEUTRINO LUMINOSITY

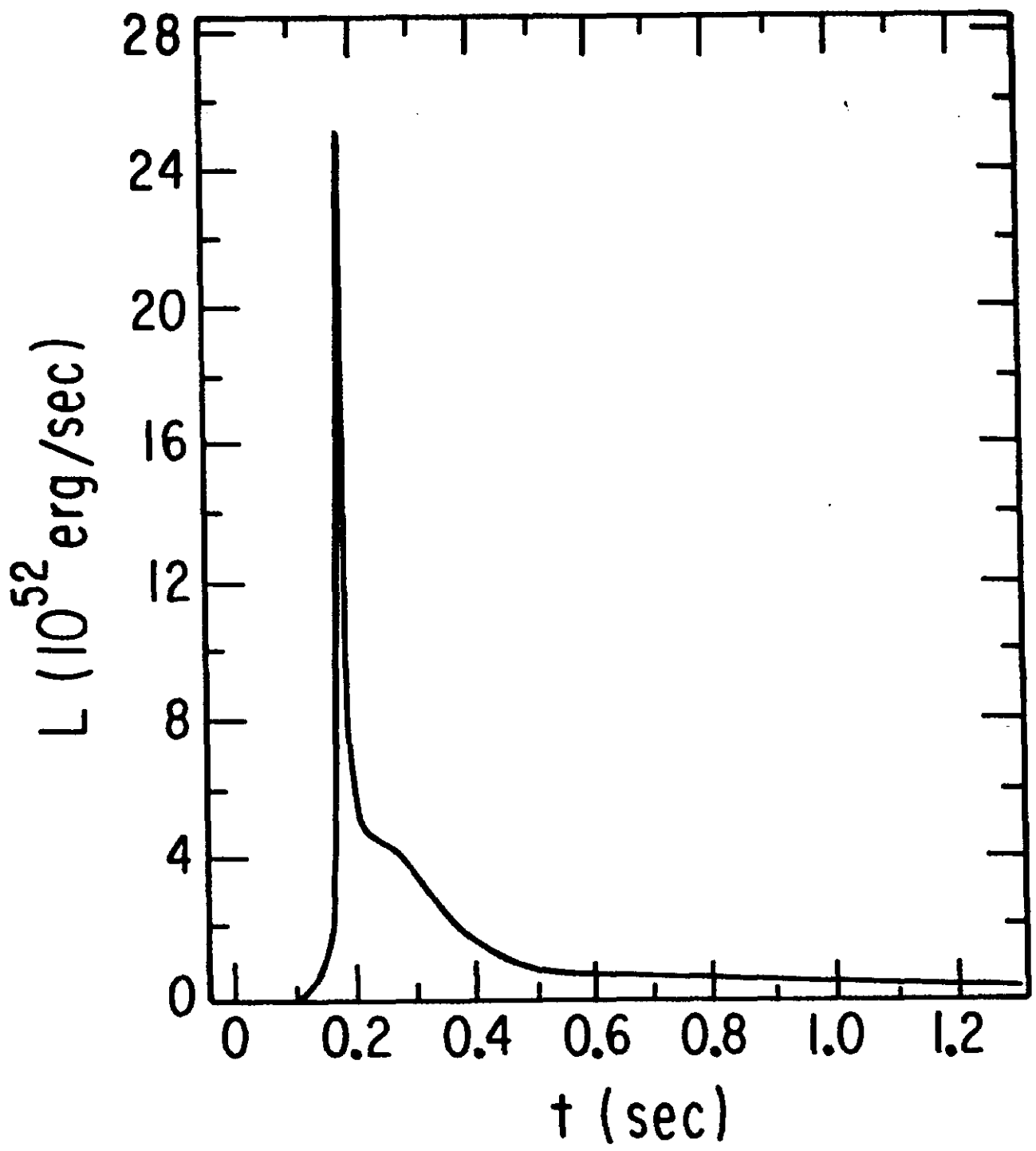


Figure 2

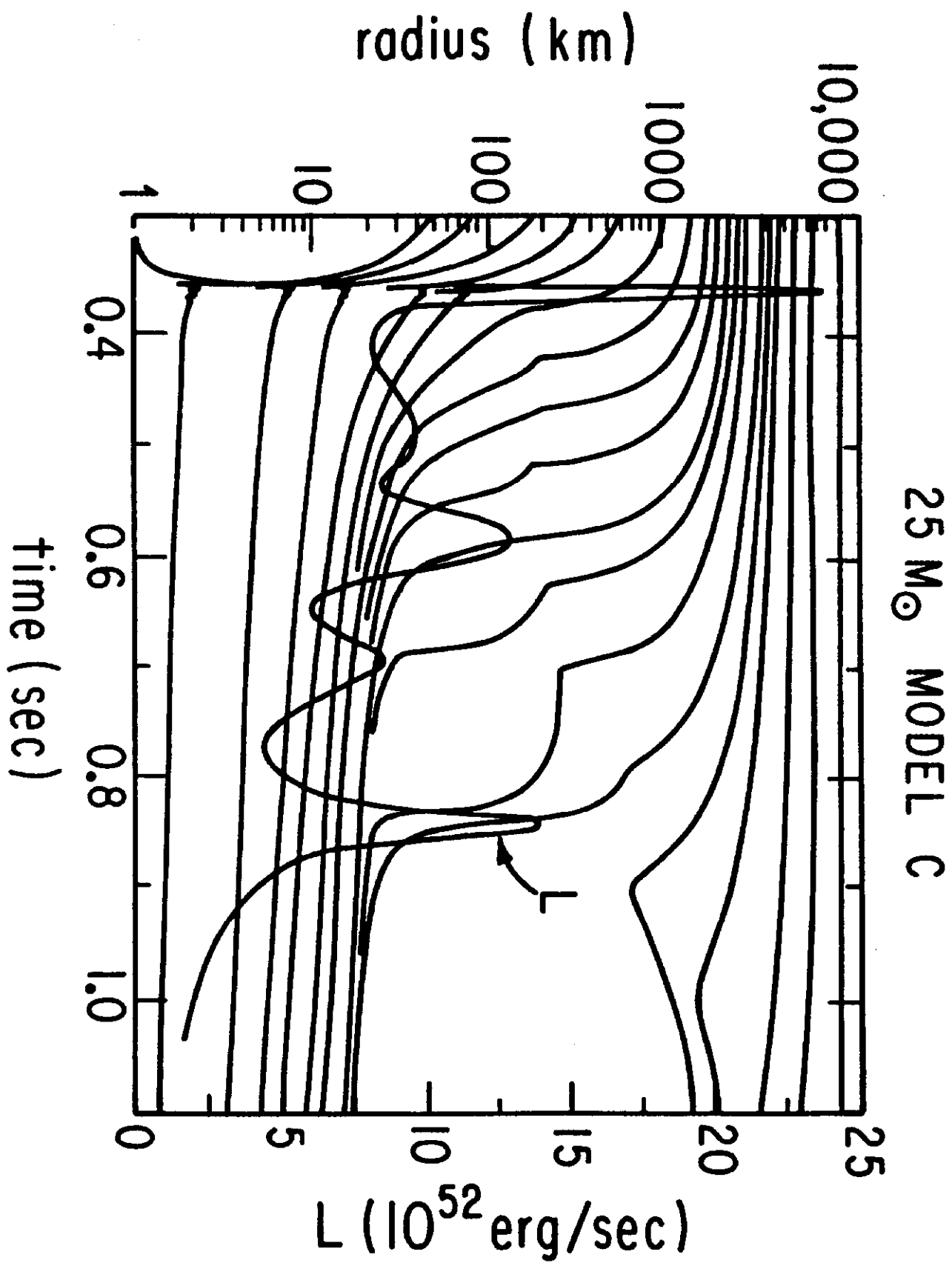


Figure 3

50 M_⊙ MODEL A ELECTRON NEUTRINO LUMINOSITY

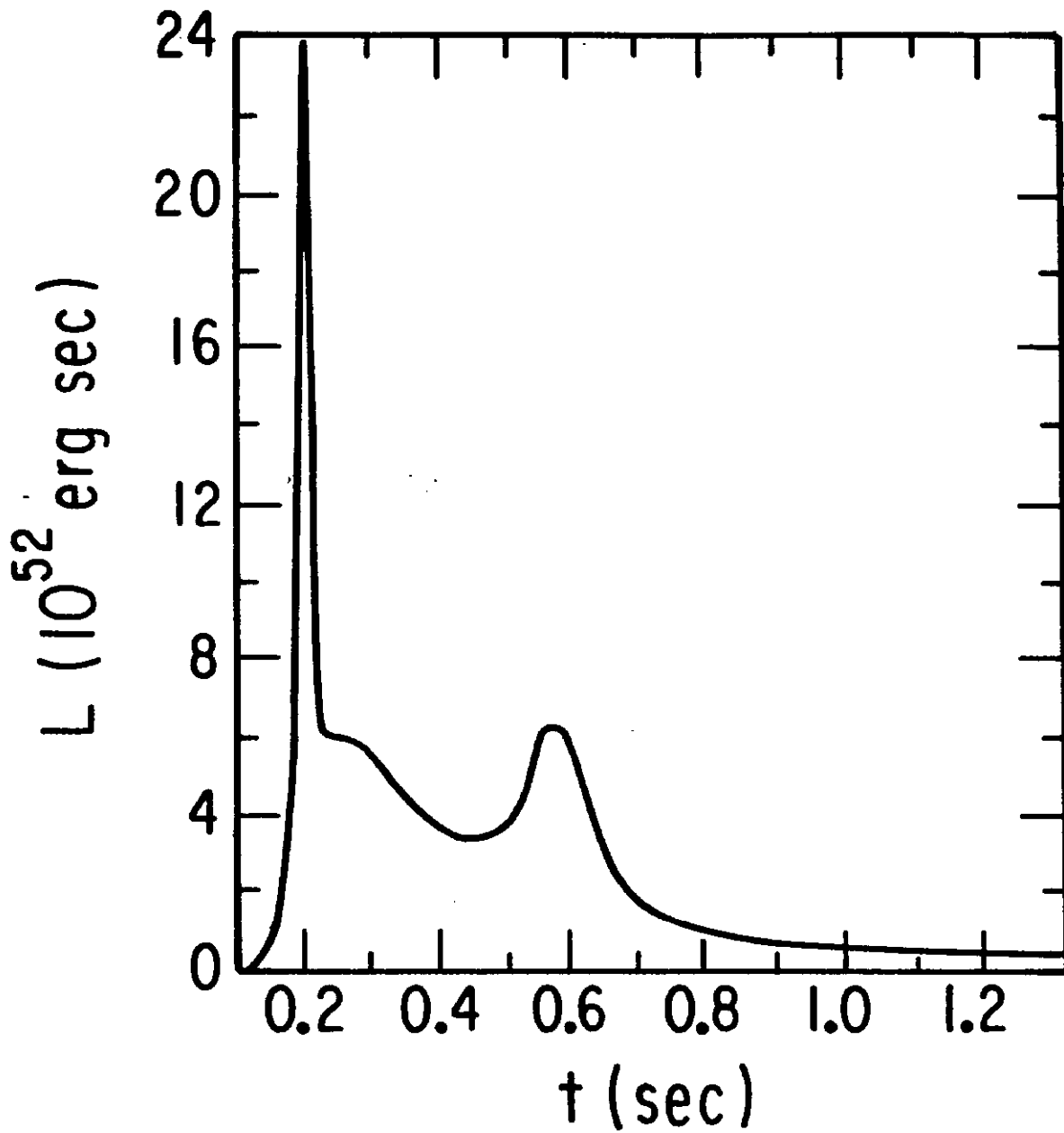


Figure 4a

100 M_⊙ MODEL A ELECTRON NEUTRINO LUMINOSITY

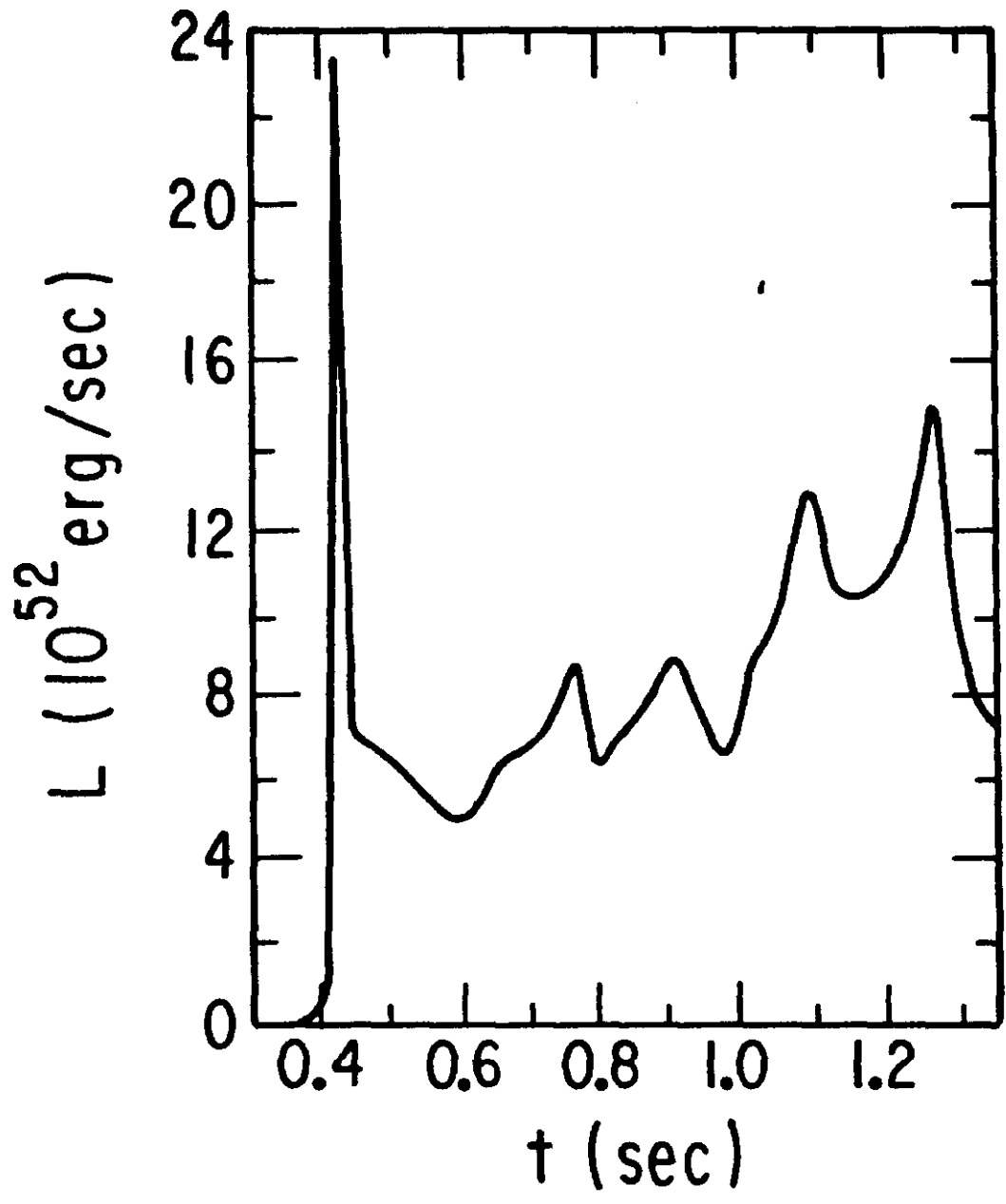


Figure 4b

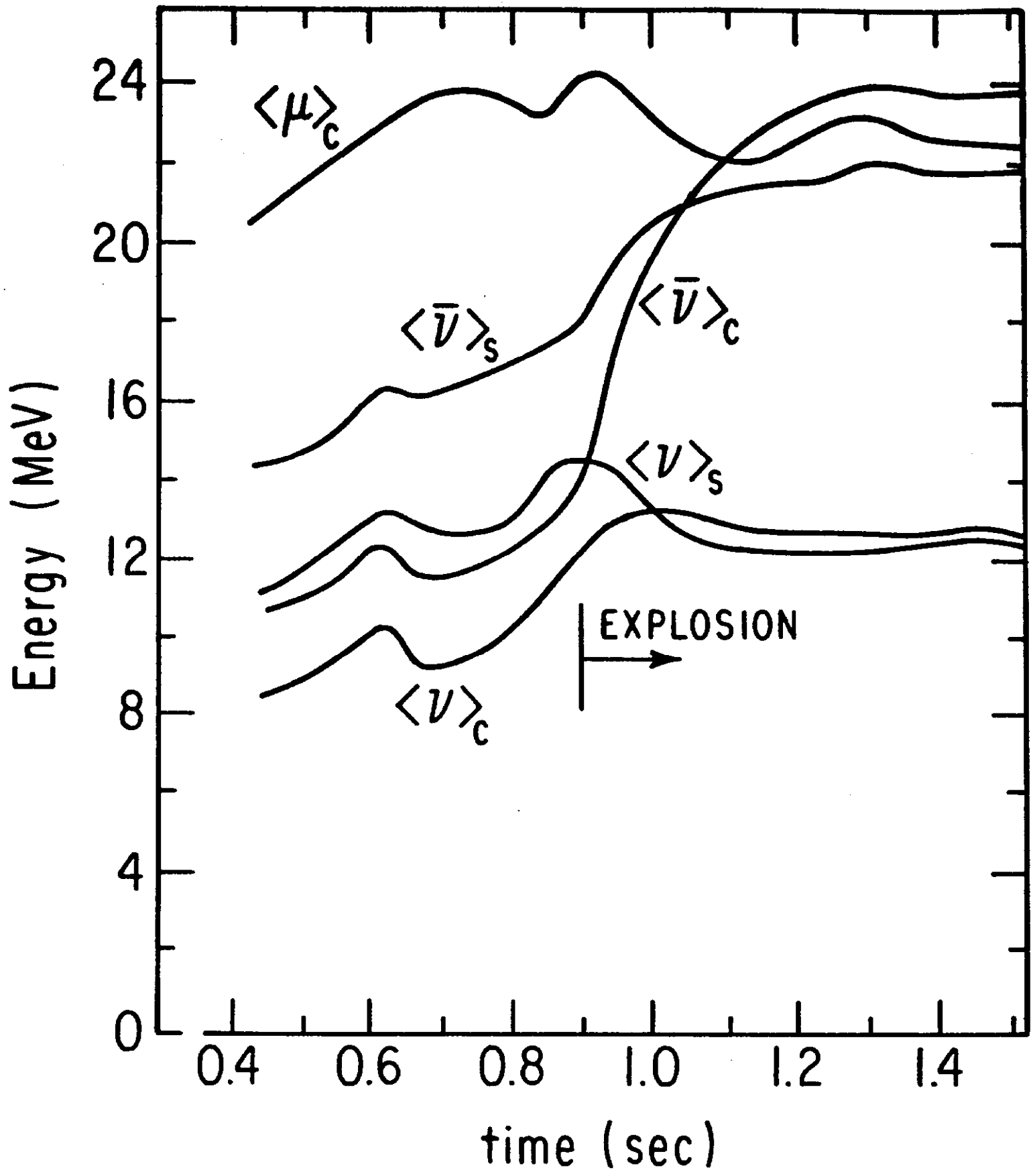


Figure 5

neut

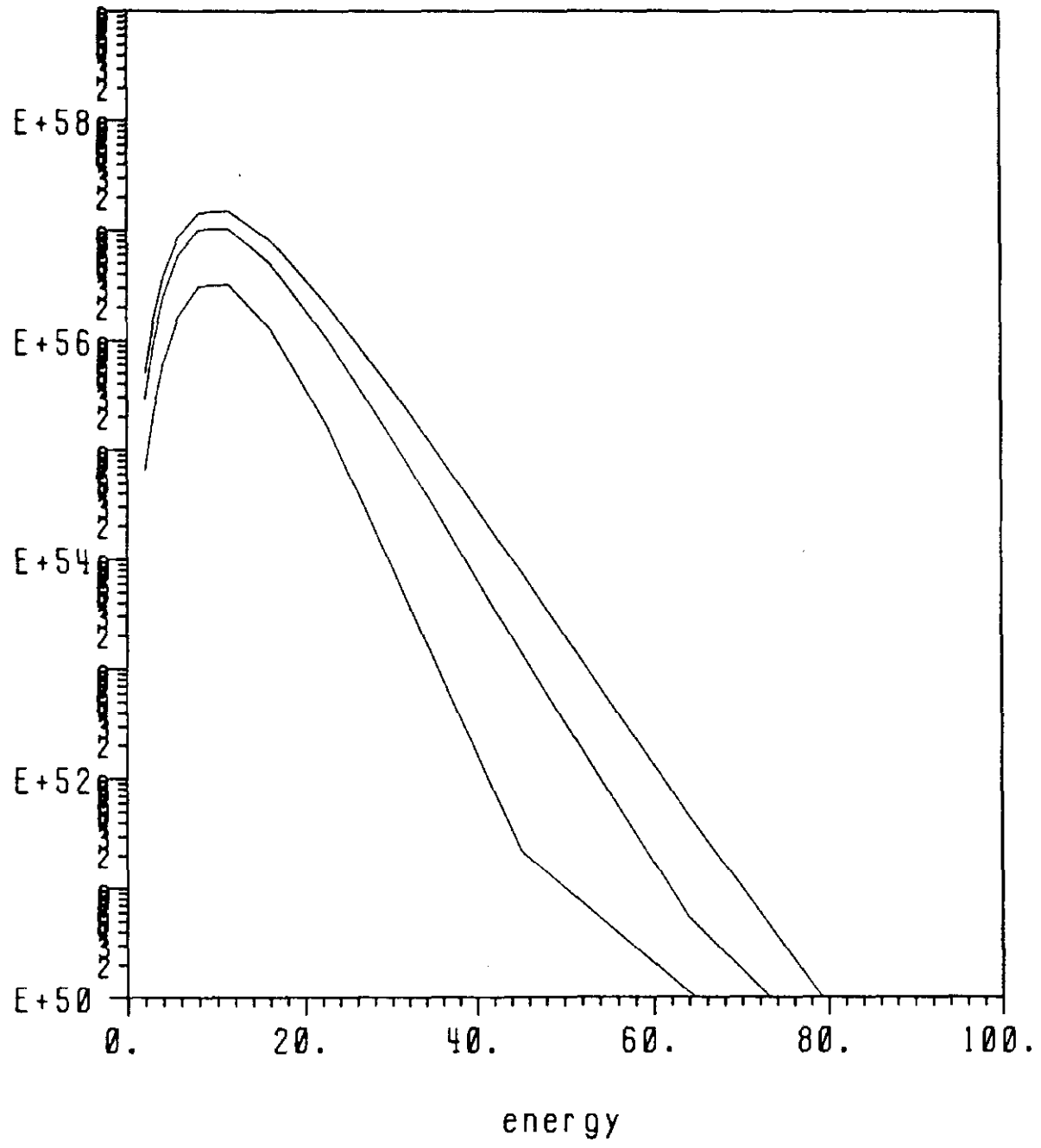
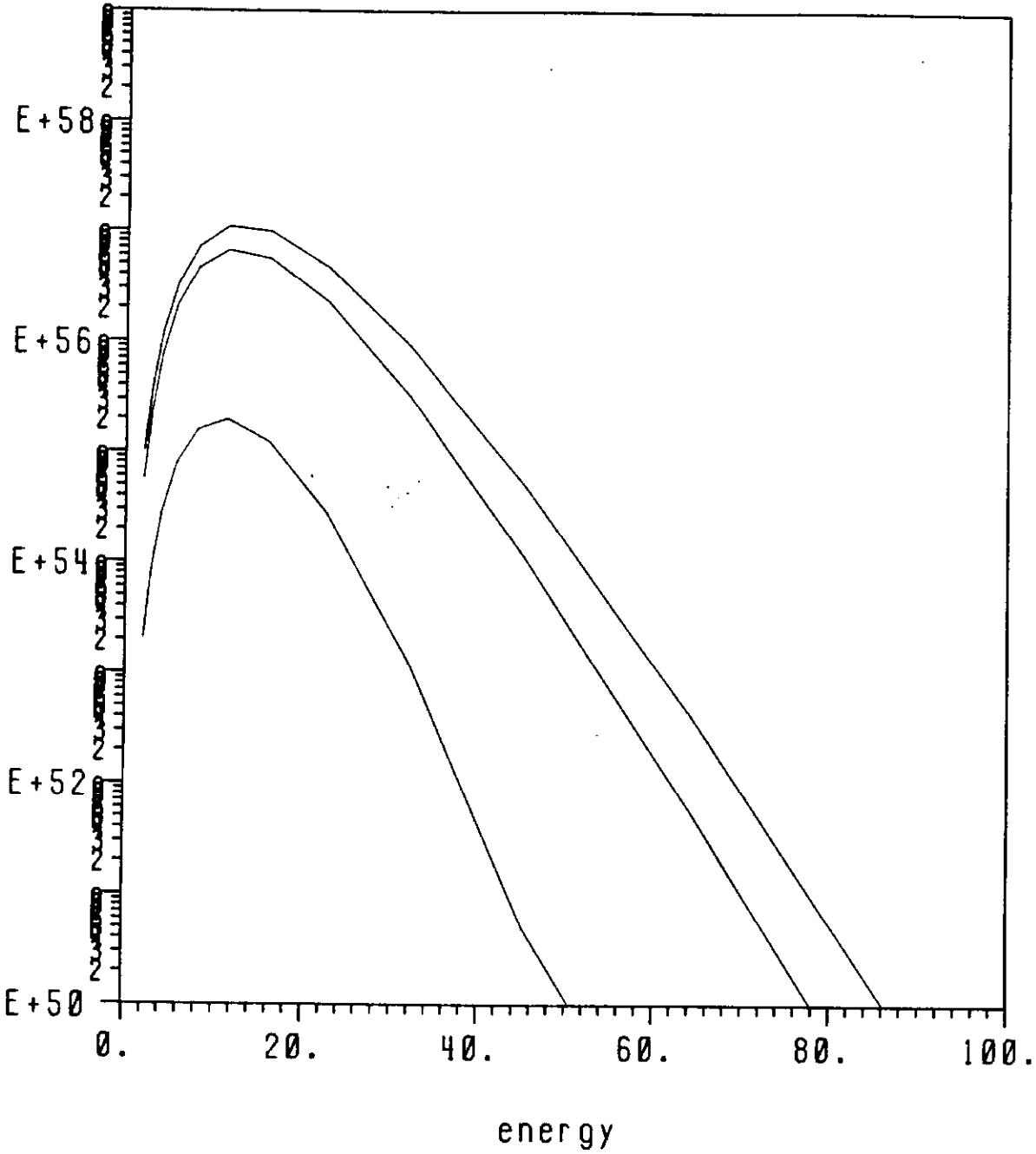


Figure 6a

anue



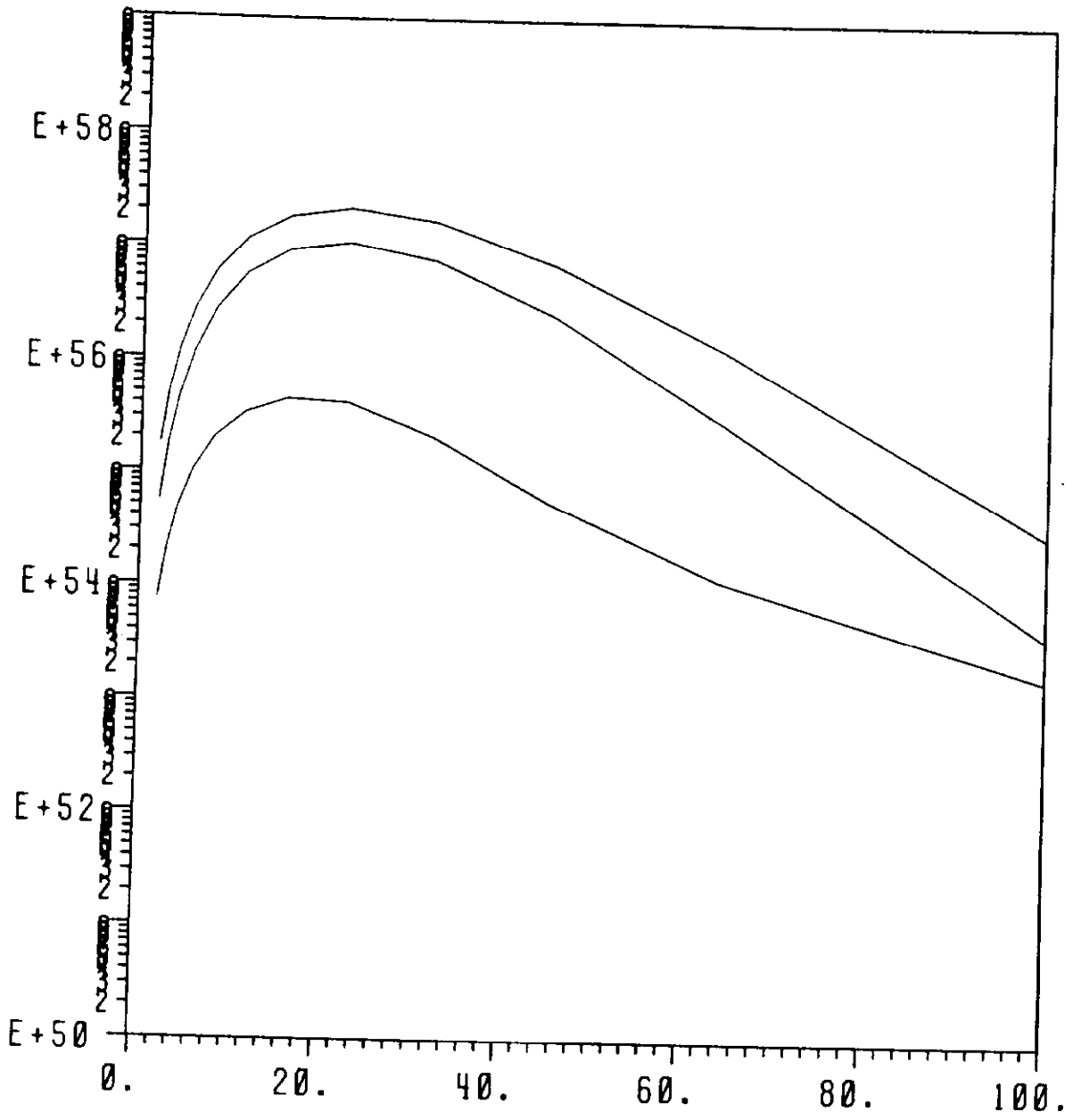
12 c
time- 5.000e-01

cyc- 3.000e+03
zone- 69

spec

Figure 6b

mutau



12 c
time: 5.000e-01
cyc: 3.000e-03
zone: 68

spec

energy

Figure 6c

neut

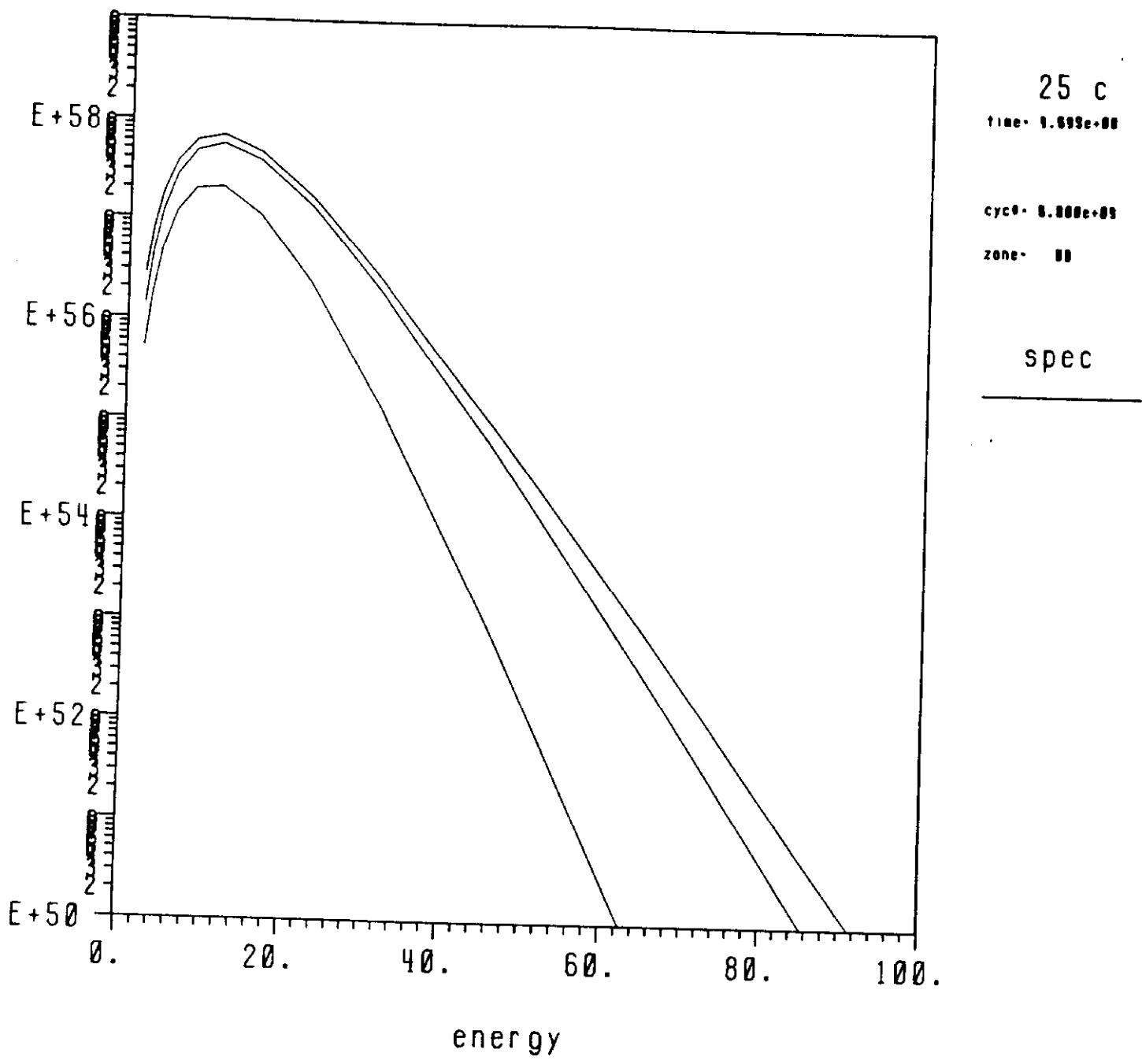


Figure 7a

anue

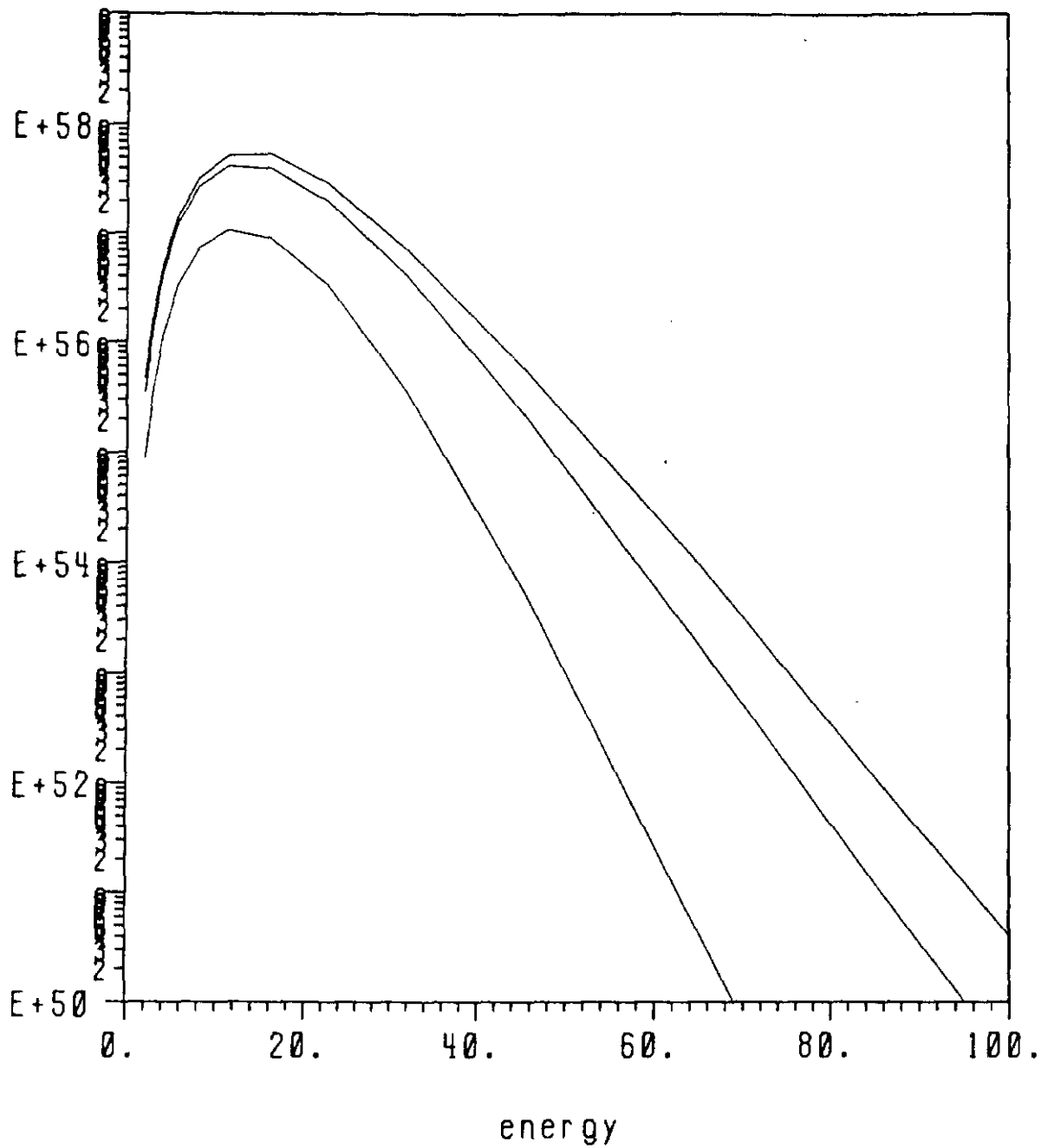
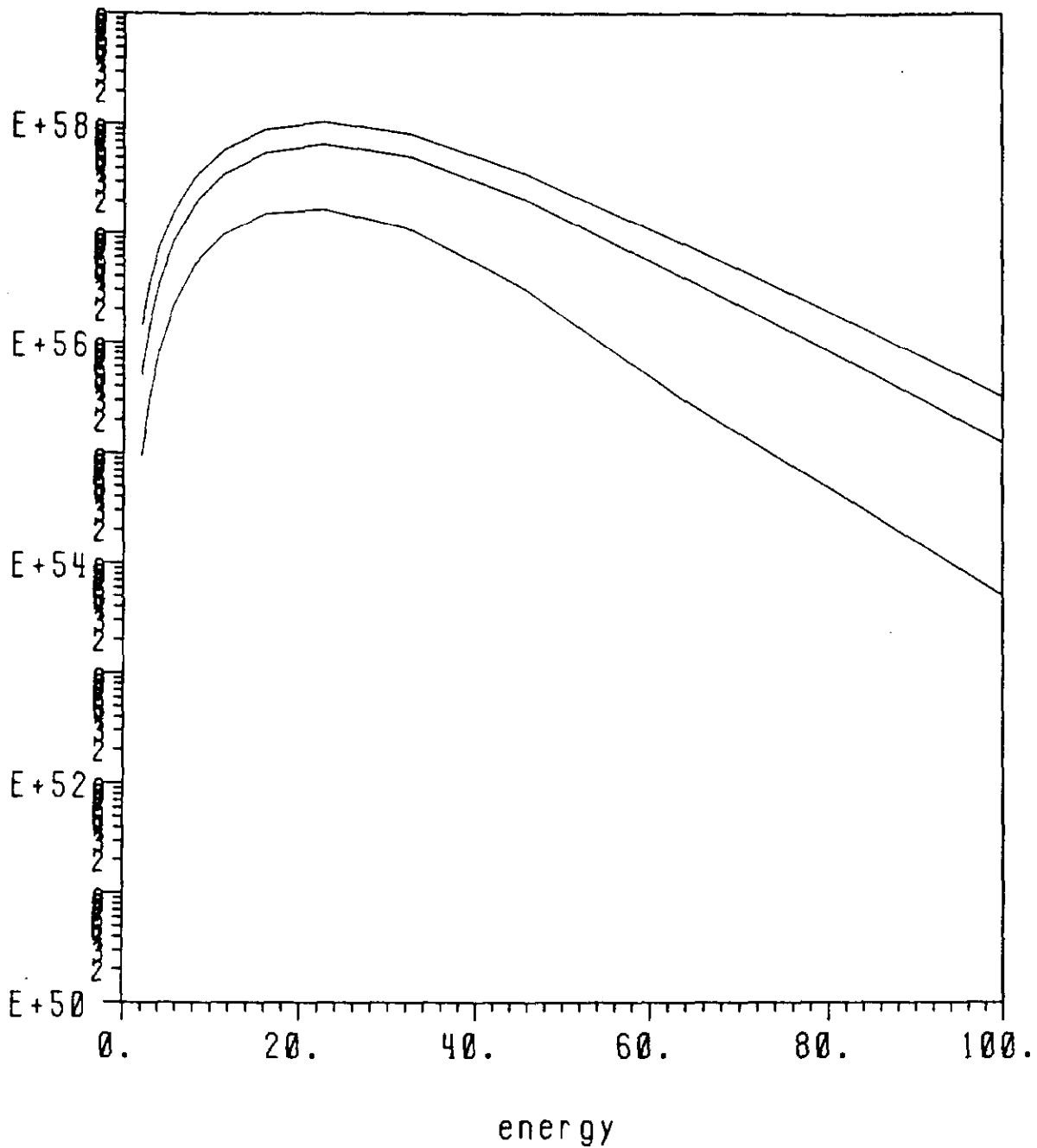


Figure 7b

mutau



25 c

time- 1.000e+00

cyc- 5.000e+03

zone- 00

spec

Figure 7c

neut

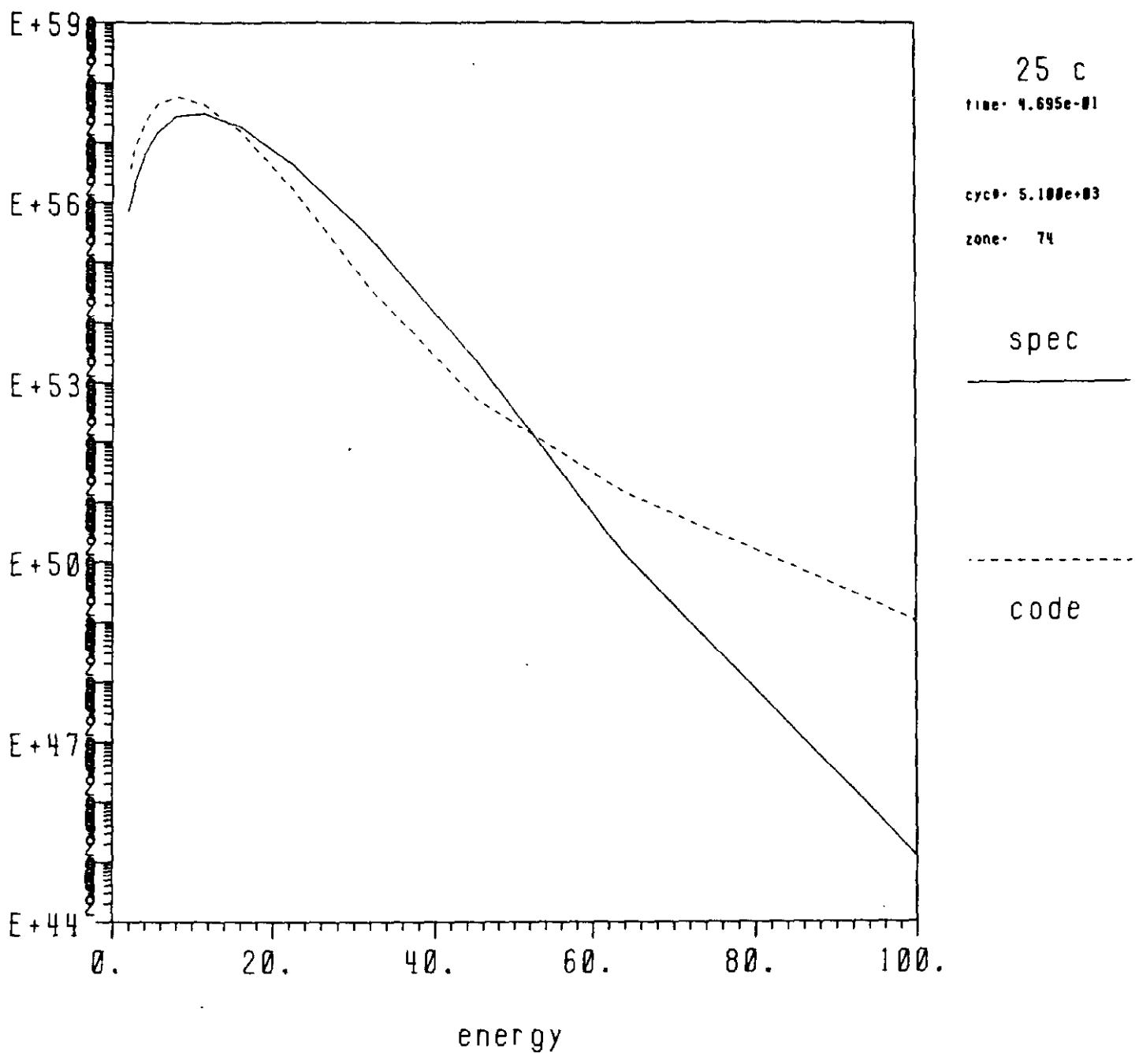


Figure 8a

neut

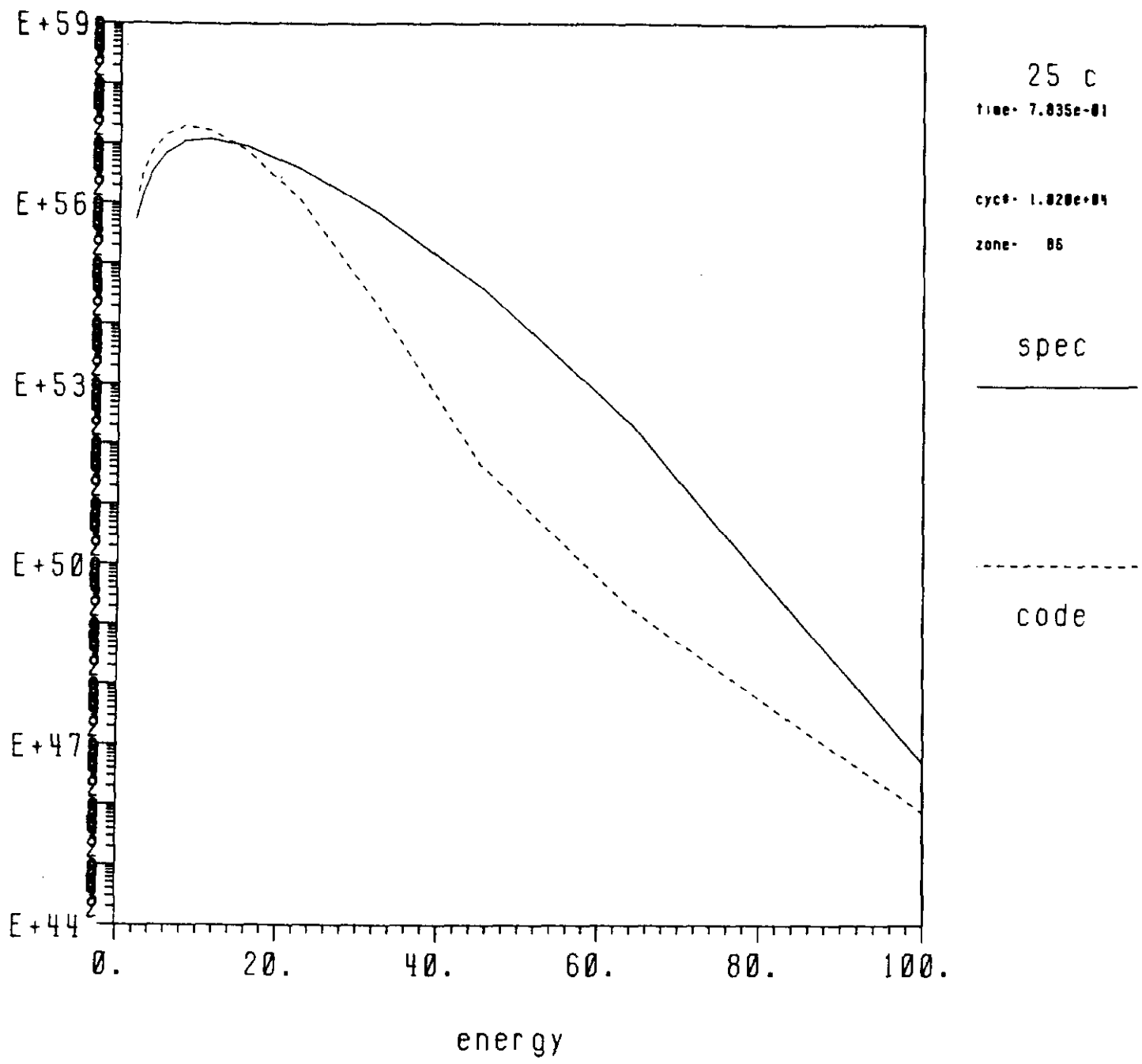


Figure 8b

neut

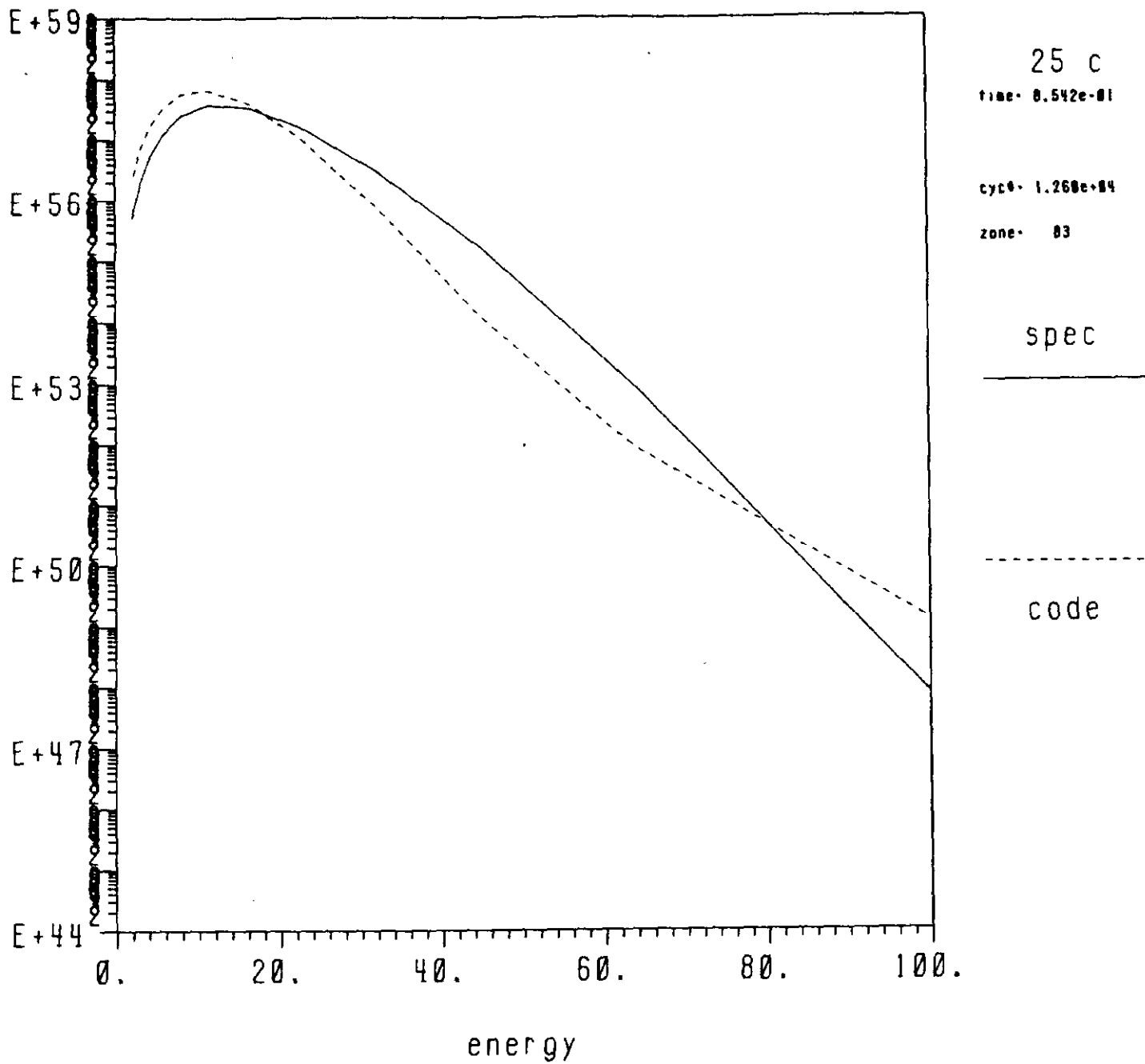


Figure 8c

neut

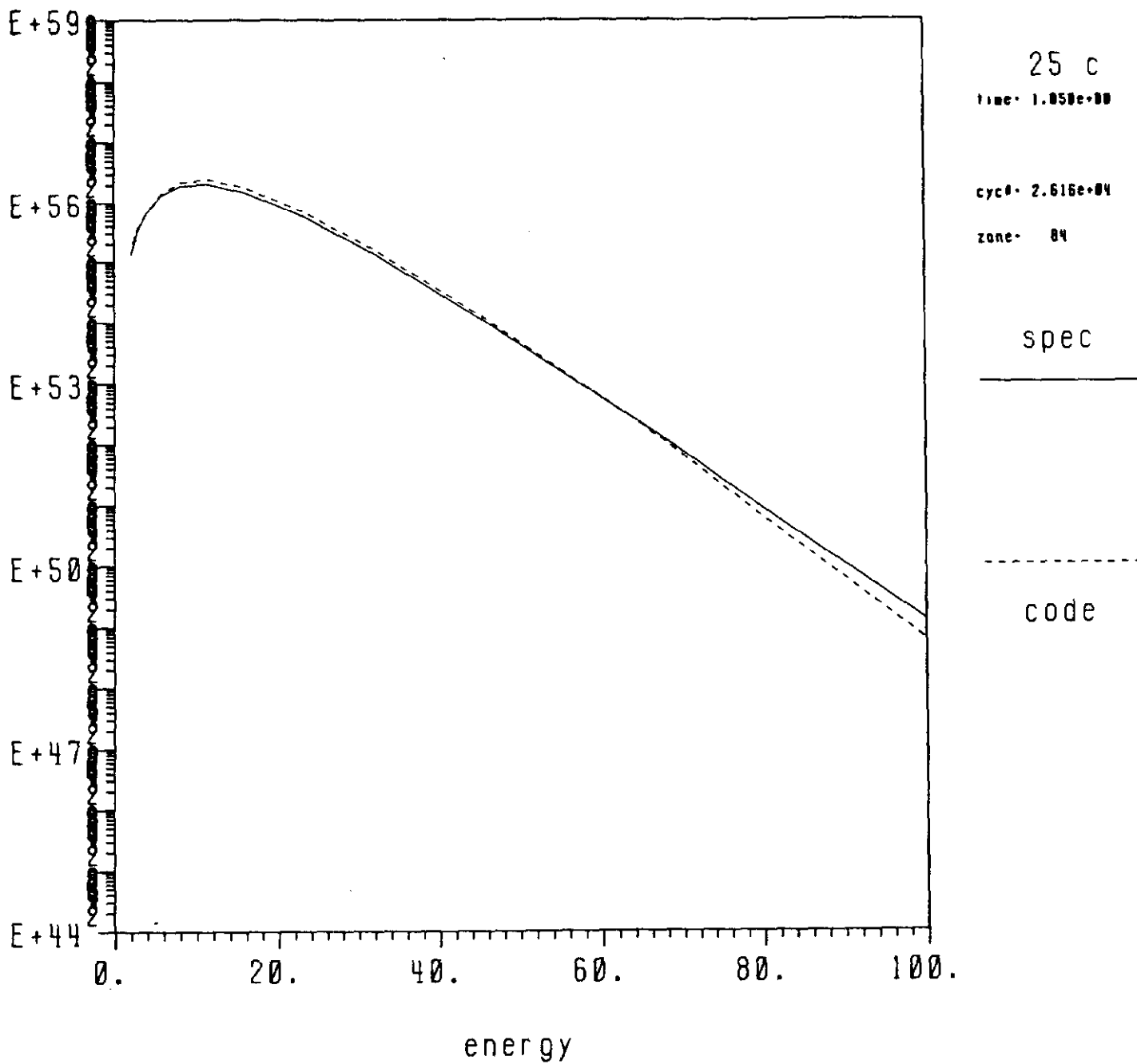


Figure 8d

neut

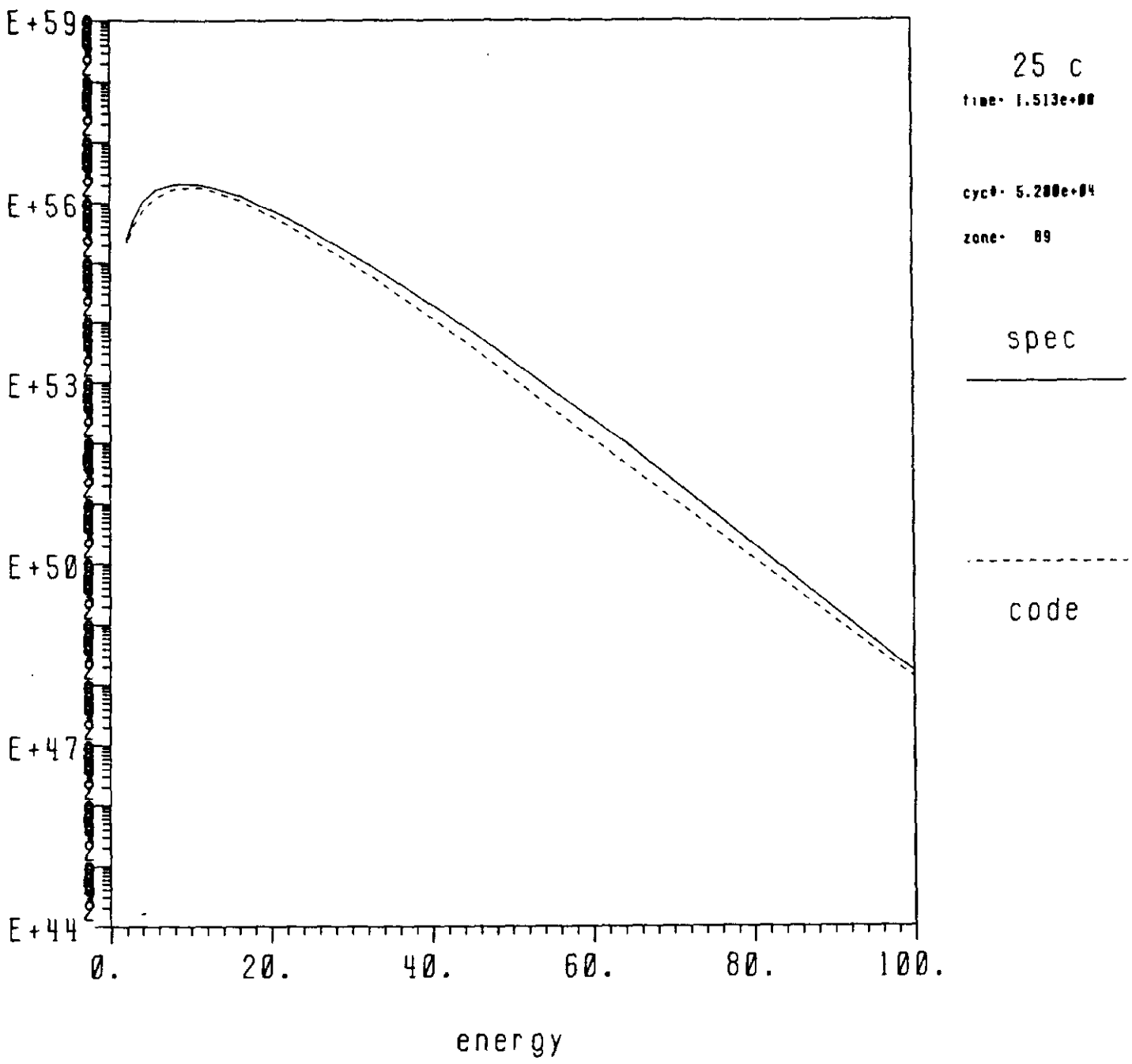


Figure 8e